
**Calculation of load capacity of bevel
gears —**

**Part 1:
Introduction and general influence
factors**

*Calcul de la capacité de charge des engrenages coniques —
Partie 1: Introduction et facteurs généraux d'influence*

STANDARDSISO.COM : Click to view the full PDF of ISO 10300-1:2023



STANDARDSISO.COM : Click to view the full PDF of ISO 10300-1:2023



COPYRIGHT PROTECTED DOCUMENT

© ISO 2023

All rights reserved. Unless otherwise specified, or required in the context of its implementation, no part of this publication may be reproduced or utilized otherwise in any form or by any means, electronic or mechanical, including photocopying, or posting on the internet or an intranet, without prior written permission. Permission can be requested from either ISO at the address below or ISO's member body in the country of the requester.

ISO copyright office
CP 401 • Ch. de Blandonnet 8
CH-1214 Vernier, Geneva
Phone: +41 22 749 01 11
Email: copyright@iso.org
Website: www.iso.org

Published in Switzerland

Contents

| | Page |
|---|-----------|
| Foreword..... | v |
| Introduction..... | vii |
| 1 Scope..... | 1 |
| 2 Normative references..... | 1 |
| 3 Terms and definitions..... | 2 |
| 4 Symbols and general subscripts..... | 2 |
| 5 Application..... | 6 |
| 5.1 Calculation methods..... | 6 |
| 5.1.1 General..... | 6 |
| 5.1.2 Method A..... | 6 |
| 5.1.3 Method B..... | 6 |
| 5.1.4 Method C..... | 6 |
| 5.2 Safety factors..... | 7 |
| 5.3 Rating factors..... | 7 |
| 5.3.1 Testing..... | 7 |
| 5.3.2 Manufacturing tolerances..... | 7 |
| 5.3.3 Implied accuracy..... | 8 |
| 5.4 Further factors to be considered..... | 8 |
| 5.4.1 General..... | 8 |
| 5.4.2 Lubrication..... | 8 |
| 5.4.3 Misalignment..... | 8 |
| 5.4.4 Deflection..... | 8 |
| 5.4.5 Materials and metallurgy..... | 8 |
| 5.4.6 Residual stress..... | 8 |
| 5.4.7 System dynamics..... | 9 |
| 5.4.8 Contact pattern..... | 9 |
| 5.4.9 Corrosion..... | 9 |
| 5.5 Further influence factors in the basic formulae..... | 9 |
| 6 External force and application factor, K_A..... | 10 |
| 6.1 Nominal tangential force, torque, power..... | 10 |
| 6.2 Variable load conditions..... | 10 |
| 6.3 Application factor, K_A | 10 |
| 6.3.1 Application factor — General..... | 10 |
| 6.3.2 Influences affecting external dynamic loads..... | 11 |
| 6.3.3 Establishment of application factors..... | 11 |
| 7 Dynamic factor, K_v..... | 11 |
| 7.1 General..... | 11 |
| 7.2 Design..... | 11 |
| 7.3 Manufacturing..... | 12 |
| 7.4 Transmission error..... | 12 |
| 7.5 Dynamic response..... | 12 |
| 7.6 Resonance..... | 13 |
| 7.6.1 General..... | 13 |
| 7.6.2 Gear blank resonance..... | 13 |
| 7.7 Calculation methods for K_v | 13 |
| 7.7.1 General comments..... | 13 |
| 7.7.2 Method A, K_{v-A} | 14 |
| 7.7.3 Method B, K_{v-B} | 14 |
| 7.7.4 Method C, K_{v-C} | 18 |
| 8 Face load factors, $K_{H\beta}$, $K_{F\beta}$..... | 20 |
| 8.1 General comments..... | 20 |

| | | |
|---|--|-----------|
| 8.2 | Method A | 20 |
| 8.3 | Method B | 21 |
| 8.4 | Method C | 21 |
| 8.4.1 | Face load factor, $K_{H\beta-C}$ | 21 |
| 8.4.2 | Local face load factor, $K_{H\beta,Y}$ | 21 |
| 8.4.3 | Face load factor, $K_{F\beta-C}$ | 22 |
| 8.4.4 | Lengthwise curvature factor for bending strength, K_{F0} | 22 |
| 9 | Transverse load factors, $K_{H\alpha}$, $K_{F\alpha}$ | 23 |
| 9.1 | General comments | 23 |
| 9.2 | Method A | 24 |
| 9.3 | Method B | 24 |
| 9.3.1 | Bevel gears having virtual cylindrical gears with contact ratio $\epsilon_{vY} \leq 2$ | 24 |
| 9.3.2 | Bevel gears having virtual cylindrical gears with contact ratio $\epsilon_{vY} > 2$ | 24 |
| 9.4 | Method C | 25 |
| 9.4.1 | General comments | 25 |
| 9.4.2 | Assumptions | 25 |
| 9.4.3 | Determination of the factors | 25 |
| 9.5 | Running-in allowance, y_α | 25 |
| Annex A (normative) Calculation of virtual cylindrical gears — Method B1 | | 27 |
| Annex B (normative) Calculation of virtual cylindrical gears — Method B2 | | 43 |
| Annex C (informative) Values for application factor, K_A | | 49 |
| Annex D (informative) Contact patterns | | 50 |
| Bibliography | | 54 |

STANDARDSISO.COM : Click to view the full PDF of ISO 10300-1:2023

Foreword

ISO (the International Organization for Standardization) is a worldwide federation of national standards bodies (ISO member bodies). The work of preparing International Standards is normally carried out through ISO technical committees. Each member body interested in a subject for which a technical committee has been established has the right to be represented on that committee. International organizations, governmental and non-governmental, in liaison with ISO, also take part in the work. ISO collaborates closely with the International Electrotechnical Commission (IEC) on all matters of electrotechnical standardization.

The procedures used to develop this document and those intended for its further maintenance are described in the ISO/IEC Directives, Part 1. In particular, the different approval criteria needed for the different types of ISO document should be noted. This document was drafted in accordance with the editorial rules of the ISO/IEC Directives, Part 2 (see www.iso.org/directives).

ISO draws attention to the possibility that the implementation of this document may involve the use of (a) patent(s). ISO takes no position concerning the evidence, validity or applicability of any claimed patent rights in respect thereof. As of the date of publication of this document, ISO had not received notice of (a) patent(s) which may be required to implement this document. However, implementers are cautioned that this may not represent the latest information, which may be obtained from the patent database available at www.iso.org/patents. ISO shall not be held responsible for identifying any or all such patent rights.

Any trade name used in this document is information given for the convenience of users and does not constitute an endorsement.

For an explanation of the voluntary nature of standards, the meaning of ISO specific terms and expressions related to conformity assessment, as well as information about ISO's adherence to the World Trade Organization (WTO) principles in the Technical Barriers to Trade (TBT), see www.iso.org/iso/foreword.html.

This document was prepared by Technical Committee ISO/TC 60, *Gears*, Subcommittee SC 2, *Gear capacity calculation*.

This third edition cancels and replaces the second edition (ISO 10300-1:2014), which has been technically revised.

The main changes are as follows:

- [Table 1](#) has been inserted in which only symbols and units used in this document are provided;
- [Table 2](#) has been inserted;
- [subclause 9.1](#) — boundary conditions for the calculation of the transverse load factors method B have been rearranged;
- [Figure 3](#) — nomogram for the determination of the resonance speed, n_{E1} , for the mating solid steel pinion/solid wheel, with $c_\gamma = 20 \text{ N}/(\text{mm} \cdot \mu\text{m})$ (for bevel gears without offset only) has been removed;
- [Figure 4](#) — dynamic factor, K_{v-C} , has been removed;
- [Figure 5](#) — transverse load factors, $K_{H\alpha-B}$ and $K_{F\alpha-B}$ has been removed;
- [Figure 6](#) — running-in allowance, y_α , of gear pairs with a tangential speed of $v_{mt2} > 10 \text{ m/s}$ has been removed;
- [Figure 7](#) — running-in allowance, y_α , of gear pairs with a tangential speed of $v_{mt2} \leq 10 \text{ m/s}$ has been removed;
- [Figure A.6](#) — transverse path of contact has been newly inserted;

— [Figure A.7](#) — general definition of length of contact lines for local geometry data has been newly inserted.

A list of all parts in the ISO 10300 series can be found on the ISO website.

Any feedback or questions on this document should be directed to the user's national standards body. A complete listing of these bodies can be found at www.iso.org/members.html.

STANDARDSISO.COM : Click to view the full PDF of ISO 10300-1:2023

Introduction

When ISO 10300:2001 (all parts) became due for its first revision, the opportunity was taken to include hypoid gears, since previously the series only allowed for calculating the load capacity of bevel gears without offset axes. The former structure is retained, i.e. three parts of the ISO 10300 series, together with ISO 6336-5, and it is intended to establish general principles and procedures for rating of bevel gears. Moreover, ISO 10300 (all parts) is designed to facilitate the application of future knowledge and developments, as well as the exchange of information gained from experience.

Several calculation methods, i.e. A, B and C, are specified, which stand for decreasing accuracy and reliability from A to C because of simplifications implemented in formulae and factors. The approximate methods in ISO 10300 (all parts) are used for preliminary estimates of gear capacity where the final details of the gear design are not yet known. More detailed methods are intended for the recalculation of the load capacity limits when all important gear data are given.

ISO 10300 (all parts) does not provide an upgraded calculation procedure as a method A, although it would be available, such as finite element or boundary element methods combined with sophisticated tooth contact analyses.

On the other hand, by means of such a computer program, a new calculation procedure for bevel and hypoid gears on the level of method B was developed and checked. It is part of the ISO 10300 series as submethod B1. Besides, if the hypoid offset, a , is zero, method B1 becomes identical to the set of proven formulae of the former version of ISO 10300:2001 (all parts).

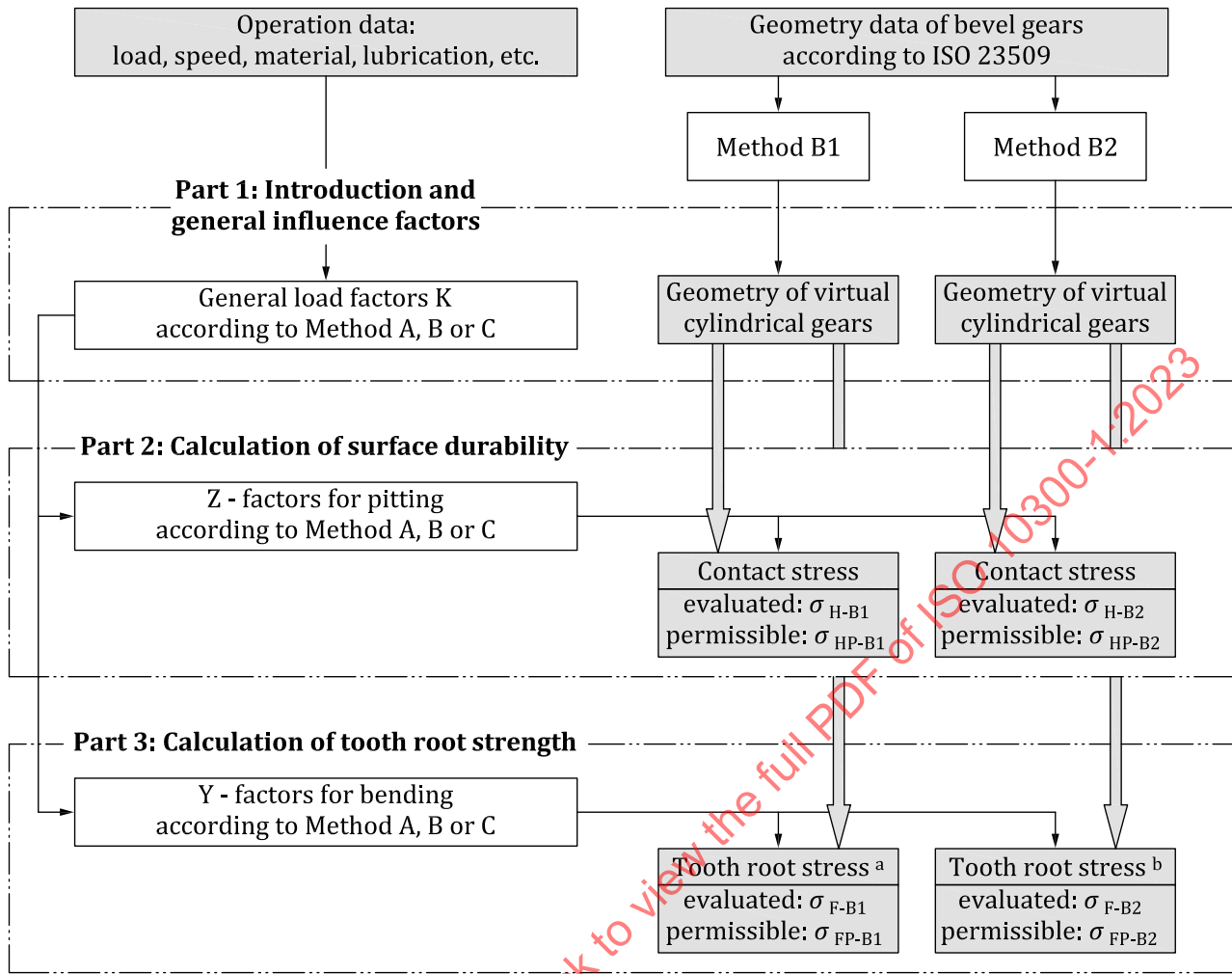
In view of the decision for ISO 10300 (all parts) to cover hypoid gears also, [Annex B](#) has been included in this document. Additionally, ISO 10300-2 is supplemented by a separate clause: “Gear flank rating formulae — Method B2”; as for ISO 10300-3, the former method B2, which uses the Lewis parabola to determine the critical section in the root and not the 30° tangent at the tooth fillet as method B1 does, is now extended by the AGMA methods for rating the strength of bevel gears and hypoid gears. It was necessary to present a new, clearer structure of the three parts, which is illustrated in [Figure 1](#).

NOTE ISO 10300 (all parts) gives no preferences in terms of when to use method B1 and when to use method B2.

The procedures covered by ISO 10300 (all parts) are based on both testing and theoretical studies.

ISO 10300 (all parts) provides calculation procedures by which different gear designs can be compared. It is not meant to ensure the performance of assembled gear drive systems. It is intended for use by the experienced gear designer capable of selecting reasonable values for the factors in these formulae, based on knowledge of similar designs and on awareness of the effects of the items discussed.

NOTE Contrary to cylindrical gears, where the contact is usually linear, bevel gears are generally manufactured with profile and lengthwise crowning, i.e. the tooth flanks are curved on all sides and the contact develops an elliptical pressure surface. This is taken into consideration when determining the load factors by the fact that the rectangular zone of action (in the case of spur and helical gears) is replaced by an inscribed parallelogram for method B1 and an inscribed ellipse for method B2 (see [Annex A](#) for method B1 and [Annex B](#) for method B2). The conditions for bevel gears, different from cylindrical gears in their contact, are thus taken into consideration by the face and transverse load distribution factors.



- ^a One set of formulae for both, bevel and hypoid gears.
- ^b Separate sets of formulae for bevel and for hypoid gears.

Figure 1 — Structure of calculation methods in ISO 10300 (all parts)

Calculation of load capacity of bevel gears —

Part 1: Introduction and general influence factors

1 Scope

This document specifies the methods of calculation of the load capacity of bevel gears, the formulae and symbols used for calculation, and the general factors influencing load conditions.

The formulae in this document are intended to establish uniformly acceptable methods for calculating the load-carrying capacity of straight, helical (skew), spiral bevel, Zerol and hypoid gears. They are applicable equally to tapered depth and uniform depth teeth. Hereinafter, the term “bevel gear” refers to all of the gear types; if not, the specific forms are identified.

The formulae in this document take into account the known major factors influencing load-carrying capacity. The rating formulae are only applicable to types of gear tooth deterioration, that are specifically addressed in the individual parts of the ISO 10300 series. Rating systems for a particular type of bevel gears can be established by selecting proper values for the factors used in the general formulae.

NOTE This document is not applicable to bevel gears which have an inadequate contact pattern under load (see [Annex D](#)).

The rating system of this document is based on virtual cylindrical gears and restricted to bevel gears whose virtual cylindrical gears have transverse contact ratios of $\varepsilon_{v\alpha} < 2$. Additionally, for bevel gears the sum of profile shift coefficients of pinion and wheel is zero (see ISO 23509).

The user is cautioned that when the formulae are used for large average mean spiral angles $(\beta_{m1} + \beta_{m2})/2 > 45^\circ$, for effective pressure angles $\alpha_e > 30^\circ$ and/or for large facewidths $b > 13 m_{mn}$, the calculated results of this document should be confirmed by experience.

2 Normative references

The following documents are referred to in the text in such a way that some or all of their content constitutes requirements of this document. For dated references, only the edition cited applies. For undated references, the latest edition of the referenced document (including any amendments) applies.

ISO 701, *International gear notation — Symbols for geometrical data*

ISO 1122-1, *Vocabulary of gear terms — Part 1: Definitions related to geometry*

ISO 6336-5, *Calculation of load capacity of spur and helical gears — Part 5: Strength and quality of materials*

ISO 6336-6, *Calculation of load capacity of spur and helical gears — Part 6: Calculation of service life under variable load*

ISO 10300-2, *Calculation of load capacity of bevel gears — Part 2: Calculation of surface durability (macropitting)*

ISO 10300-3, *Calculation of load capacity of bevel gears — Part 3: Calculation of tooth root strength*

ISO 17485, *Bevel gears — ISO system of accuracy*

ISO 23509:2016, *Bevel and hypoid gear geometry*

3 Terms and definitions

For the purposes of this document, the terms and definitions given in ISO 1122-1 and ISO 23509 apply.

ISO and IEC maintain terminology databases for use in standardization at the following addresses:

- ISO Online browsing platform: available at <https://www.iso.org/obp>
- IEC Electropedia: available at <https://www.electropedia.org/>

4 Symbols and general subscripts

For the purposes of this document, the symbols given in ISO 701, ISO 17485, ISO 23509, and the following shall apply. See [Tables 1](#) and [2](#).

Table 1 — Symbols

| Symbol | Description or term | Unit |
|----------------|---|-----------|
| A | Auxiliary factor for calculating the dynamic factor K_{v-c} | — |
| A^* | Related area for calculating the load sharing factor Z_{LS} | mm |
| a | Hypoid offset | mm |
| a_{rel} | Relative hypoid offset | — |
| a_v | Centre distance of virtual cylindrical gear pair | mm |
| a_{vn} | Relative centre distance of virtual cylindrical gear pair in normal section | — |
| B | Accuracy grade according to ISO 17485 | — |
| b | Facewidth | mm |
| b_{ce} | Calculated effective facewidth | mm |
| b_{eff} | Effective facewidth (e.g. measured length of contact pattern) | mm |
| b_v | Facewidth of virtual cylindrical gears | mm |
| $b_{v,eff}$ | Effective facewidth of virtual cylindrical gears | mm |
| $b_{v,rel}$ | Relative facewidth of virtual cylindrical gear | — |
| C_F | Correction factor of tooth stiffness for non-average conditions | — |
| C_{lb} | Correction factor for the length of contact lines | — |
| c_v | Empirical parameter to determine the dynamic factor | — |
| c_γ | Mean value of mesh stiffness per unit facewidth | N/(mm·µm) |
| $c_{\gamma 0}$ | Mesh stiffness for average conditions | N/(mm·µm) |
| c' | Single stiffness | N/(mm·µm) |
| c_0' | Single stiffness for average conditions | N/(mm·µm) |
| d_e | Outer pitch diameter | mm |
| d_m | Mean pitch diameter | mm |
| d_T | Tolerance diameter according to ISO 17485 | mm |
| d_v | Reference diameter of virtual cylindrical gear | mm |
| d_{va} | Tip diameter of virtual cylindrical gear | mm |
| d_{van} | Tip diameter of virtual cylindrical gear in normal section | mm |
| d_{vb} | Base diameter of virtual cylindrical gear | mm |
| d_{vbn} | Base diameter of virtual cylindrical gear in normal section | mm |
| d_{vf} | Root diameter of virtual cylindrical gear | mm |
| d_{vn} | Reference diameter of virtual cylindrical gear in normal section | mm |

Table 1 (continued)

| Symbol | Description or term | Unit |
|-----------------|---|-------------------|
| E | Modulus of elasticity, Young's modulus | N/mm ² |
| e_{LS} | Exponent for the load distribution along the lines of contact | — |
| F_{mt} | Nominal tangential force at mid-facewidth of the reference cone | N |
| F_{mtH} | Determinant tangential force at mid-facewidth of the reference cone | N |
| F_{vmt} | Nominal tangential force of virtual cylindrical gears | N |
| f | Distance from the centre of the zone of action to a contact line | mm |
| f_m | Distance of the middle contact line in the zone of action | mm |
| $f_{m,Y}$ | Distance of the middle contact line in the zone of action for a contact point Y | mm |
| f_{max} | Maximum distance to middle contact line | mm |
| f_{maxB} | Maximum distance to middle contact line at right side of contact pattern | mm |
| f_{max0} | Maximum distance to middle contact line at left side of contact pattern | mm |
| f_{pt} | Single pitch deviation | µm |
| $f_{p,eff}$ | Effective pitch deviation | µm |
| f_r | Distance of the root contact line in the zone of action | mm |
| $f_{r,Y}$ | Distance of the root contact line in the zone of action for a contact point Y | mm |
| f_t | Distance of the tip contact line in the zone of action | mm |
| $f_{t,Y}$ | Distance of the tip contact line in the zone of action for a contact point Y | mm |
| g_{va} | Length of path of contact | mm |
| $g_{va\alpha}$ | Length of path of contact of virtual cylindrical gear in transverse section | mm |
| g_{van} | Relative length of action in normal section | — |
| g_{vana} | Relative length of action from pinion tip to pitch circle in the normal section | — |
| g_{vanr} | Relative length of action from wheel tip to pitch circle in the normal section | — |
| g_η | Relative length of action within the contact ellipse | — |
| h_{am} | Mean addendum | mm |
| h_{fm} | Mean dedendum | mm |
| h_{vfm} | Relative mean virtual dedendum | — |
| i | Run variable | — |
| K | Constant; factor for calculating the dynamic factor $K_{v,B}$ | — |
| K_v | Dynamic factor | — |
| K_v^* | Preliminary dynamic factor for non-hypoid gears | — |
| K_A | Application factor | — |
| K_{F0} | Lengthwise curvature factor for bending stress | — |
| $K_{F\alpha}$ | Transverse load factor for bending stress | — |
| $K_{F\beta}$ | Face load factor for bending stress | — |
| $K_{H\alpha}$ | Transverse load factor for contact stress | — |
| $K_{H\alpha}^*$ | Preliminary transverse load factor for contact stress for non-hypoid gears | — |
| $K_{H\beta}$ | Face load factor for contact stress | — |
| $K_{H\beta-be}$ | Mounting factor | — |
| k_S | Correction factor | — |
| k' | Contact shift factor | — |
| l_b | Length of contact line (method B1) | mm |
| l_{b0} | Theoretical length of contact line | mm |
| m_{et} | Outer transverse module | mm |
| m_{mn} | Mean normal module | mm |

Table 1 (continued)

| Symbol | Description or term | Unit |
|-----------------|--|-------------------|
| m_{red} | Mass per unit facewidth reduced to the line of action of dynamically equivalent cylindrical gear pairs | kg/mm |
| m_{vt} | Transverse module | mm |
| m^* | Relative individual gear mass per unit facewidth referred to line of action | kg/mm |
| N | Reference speed related to resonance speed n_{E1} | — |
| n | Rotational speed | min ⁻¹ |
| n_{E1} | Resonance speed of pinion | min ⁻¹ |
| P | Nominal power | kW |
| p | Peak load | N/mm |
| p^* | Relative peak load for calculating the load sharing factor (method B1) | — |
| p_{mn} | Relative mean normal pitch | — |
| p_{vet} | Transverse base pitch of virtual cylindrical gear (method B1) | mm |
| q | Exponent in the Formula for lengthwise curvature factor | — |
| R_m | Mean cone distance | mm |
| R_{mpt} | Relative mean back cone distance | — |
| r_{c0} | Cutter radius | mm |
| r_{va} | Relative mean virtual tip radius | — |
| r_{vbn} | Relative mean virtual base radius | — |
| r_{vn} | Relative mean virtual pitch radius | — |
| s_{mn} | Mean normal circular thickness | mm |
| s_{vmn} | Relative virtual tooth thickness | — |
| $T_{1,2}$ | Nominal torque of pinion and wheel | Nm |
| u | Gear ratio of bevel gear | — |
| u_v | Gear ratio of virtual cylindrical gear | — |
| v_{et} | Tangential speed at outer end (heel) of the reference cone | m/s |
| $v_{et,max}$ | Maximum pitch line velocity at operating pitch diameter | m/s |
| v_{mt} | Tangential speed at mid-facewidth of the reference cone | m/s |
| X_Y | Curvature factor | — |
| x | Coordinates of the ends of the contact line | mm |
| Y_{FS} | Combined tooth form factor for generated gears | — |
| Y_{LS} | Load sharing factor (bending) | — |
| y_p | Running-in allowance for pitch deviation related to the polished test piece | µm |
| y_α | Running-in allowance for pitch deviation | µm |
| Z_{LS} | Load sharing factor (method B1) | — |
| z | Number of teeth | — |
| z_v | Number of teeth of virtual cylindrical gear | — |
| z_{vn} | Number of teeth of virtual cylindrical gear in normal section | — |
| z_Y | Auxiliary value | mm |
| z_0 | Number of blade groups of the cutter | — |
| α_a | Adjusted pressure angle (method B2) | ° |
| $\alpha_{eD,C}$ | Effective pressure angle for drive side/coast side | ° |
| α_{et} | Effective pressure angle in transverse section | ° |
| α_{lim} | Limit pressure angle | ° |
| $\alpha_{nD,C}$ | Generated pressure angle for drive side/coast side | ° |

Table 1 (continued)

| Symbol | Description or term | Unit |
|----------------------|---|--------------------|
| α_{vet} | Effective pressure angle of virtual cylindrical gears calculated for the active flank | ° |
| β_B | Inclination angle of contact line | ° |
| β_m | Mean spiral angle | ° |
| β_v | Helix angle of virtual gear (method B1), virtual spiral angle (method B2) | ° |
| β_{vb} | Helix angle at base circle of virtual cylindrical gear | ° |
| γ | Auxiliary angle for length of contact line calculation (method B1) | ° |
| γ' | Projected auxiliary angle for length of contact line | ° |
| δ | Pitch angle of bevel gear | ° |
| δ_a | Face angle | ° |
| δ_f | Root angle | ° |
| ϵ_N | Load sharing ratio for bending (method B2) | — |
| $\epsilon_{v\alpha}$ | Transverse contact ratio of virtual cylindrical gears | — |
| ϵ_{van} | Transverse contact ratio of virtual cylindrical gears in normal section | — |
| $\epsilon_{v\beta}$ | Face contact ratio of virtual cylindrical gears | — |
| $\epsilon_{v\gamma}$ | Virtual contact ratio (method B1), modified contact ratio (method B2) | — |
| η | Auxiliary angle | ° |
| ζ_R | Pinion offset angle in root plane | ° |
| ζ_m | Pinion offset angle in axial plane | ° |
| ζ_{mp} | Pinion offset angle in pitch plane | ° |
| θ_{v2} | Angular pitch of virtual cylindrical wheel | rad |
| ϑ_{mp} | Auxiliary angle for virtual facewidth (method B1) | ° |
| λ | Adjustment angle for contact angle of hypoid gears (method B2) | ° |
| λ_r | Adjustment angle for virtual spiral angle of hypoid gears (method B2) | ° |
| ρ | Density of gear material | kg/mm ³ |
| ρ_{a0} | Cutter edge radius | mm |
| $\rho_{m\beta}$ | Lengthwise tooth mean radius of curvature | mm |
| ρ_{rel} | Local equivalent radius of curvature vertical to the contact line | mm |
| ρ_t | Relative radius of profile curvature between pinion and wheel (method B2) | — |
| ρ_{va0} | Relative edge radius of tool | — |
| ρ' | Slip layer thickness | mm |
| $\sigma_{H,lim}$ | Allowable stress number for contact stress | N/mm ² |
| v_0 | Lead angle of face hobbing cutter | ° |
| φ | Auxiliary angle to determine the position of the pitch point | ° |
| ω | Angular velocity | rad/s |
| Σ | Shaft angle | ° |

Table 2 — General subscripts

| Subscripts | Description |
|-----------------|---|
| 0 | Tool |
| 1 | Pinion |
| 2 | Wheel |
| A, B, B1, B2, C | Value according to method A, B, B1, B2 or C |
| D | Drive flank |
| C | Coast flank |
| T | Relative to standardized test gear dimensions |
| (1), (2) | Trials of interpolation |

5 Application

5.1 Calculation methods

5.1.1 General

ISO 10300 (all parts) provides the procedures to predict load capacity of bevel gears. The most valid method is full-scale and full-load testing of a specific gear set design. However, at the design stage or in certain fields of application, some calculation methods are needed to predict load capacity. Therefore, methods A, B and C are used in this document, while method A, if its accuracy and reliability are proven, is preferred over method B, which in turn is preferred over method C.

ISO 10300 (all parts) allows the use of mixed factor rating methods within method B1 or method B2. For example, method B for dynamic factor K_{v-B} may be used with method C face load factor $K_{H\beta-C}$.

For the calculation of the virtual cylindrical gear geometry, [Annex A](#) shall apply for method B1 and [Annex B](#) shall apply for method B2.

5.1.2 Method A

Where sufficient experience from the operation of other, similar designs is available, satisfactory guidance can be obtained by the extrapolation of the associated test results or field data. The factors involved in this extrapolation may be evaluated by the precise measurement and comprehensive mathematical analysis of the transmission system under consideration, or from field experience. All gear and load data shall be known for the use of this method, which shall be clearly described and presented with all mathematical and test premises, boundary conditions and any specific characteristics of the method that influence the result. The accuracy and the reliability of the method shall be demonstrated. Precision, for example, shall be demonstrated through comparison with other, acknowledged gear measurements. The method should be approved by both the customer and the supplier.

5.1.3 Method B

Method B provides the calculation formulae to predict load capacity of bevel gears for which the essential data are known. However, sufficient experience from the operation of other, similar designs is needed in the evaluation of certain factors even in this method. The validity of these evaluations for the given operating conditions shall be checked.

5.1.4 Method C

Where suitable test results or field experience from similar designs are unavailable for use in the evaluation of certain factors, a further simplified calculation method, method C, should be used.

5.2 Safety factors

The allowable probability of failure shall be carefully weighed when choosing a safety factor, in balancing reliability against cost. If the performance of the gears can be accurately appraised by testing the unit itself under actual load conditions, lower safety factors are allowed. The safety factors shall be determined by dividing the calculated permissible stress by the specific evaluated operating stress.

In addition to this general requirement and the special requirements relating to surface durability (macropitting) and tooth root strength (see ISO 10300-2 and ISO 10300-3, respectively), safety factors shall be determined only after careful consideration of the reliability of the material data and of the load values used for calculation. The allowable stress numbers used for calculation are valid for a given probability of failure, or damage (the material values in ISO 6336-5, for example, are valid for a 1 % probability of damage), the risk of damage being reduced as the safety factors are increased, and vice versa. If loads, or the response of the system to vibration, are estimated rather than measured, a larger factor of safety should be used.

The following deviations shall also be taken into consideration in the determination of a safety factor:

- deviations in gear geometry due to manufacturing;
- deviations in alignment of gear members;
- variations in material due to process variations in chemistry, cleanliness and microstructure (material quality and heat treatment);
- variations in lubrication and its maintenance over the service life of the gears.

The appropriateness of the safety factors will thus depend on the reliability of the assumptions, such as those related to load, on which the calculations are based, as well as on the reliability required of the gears themselves, in respect of the possible consequences of any damage that can occur in the case of failure.

Supplied gears or assembled gear drives should have a minimum safety factor for contact stress $S_{H,min}$ of 1,0. The minimum bending stress value $S_{F,min}$ should be 1,3 for spiral bevel including hypoid gears, and 1,5 for straight bevel gears or those with $\beta_m \leq 5^\circ$.

The minimum safety factors against macropitting damage and tooth breakage should be agreed between the supplier and customer.

5.3 Rating factors

5.3.1 Testing

The most effective overall approach to gear system performance management is through the full-scale, full-load testing of a proposed new design. Alternatively, where sufficient experience of similar designs exists and results are available, a satisfactory solution may be obtained through extrapolation from such data. On the other hand, where suitable test results or field data are not available, rating factor values should be chosen conservatively.

5.3.2 Manufacturing tolerances

Rating factors should be evaluated based on the acceptable quality limits of the expected variation of parts in the manufacturing process. The accuracy grade, B, shall be determined, preferably as specified in ISO 17485, e.g. single pitch deviation for calculating the dynamic factor K_{V-B} .

5.3.3 Implied accuracy

Where the empirical values for rating factors are given by curves, this document provides curve fitting equations to facilitate computer programming.

NOTE The constants and coefficients used in curve fitting often have significant digits in excess of those implied by the reliability of the empirical data.

5.4 Further factors to be considered

5.4.1 General

In addition to the factors considered that influence macropitting resistance and bending strength, other interrelated system factors can have an important effect on overall transmission performance. Their possible effect on the calculations should be considered.

5.4.2 Lubrication

The ratings determined by the formulae of ISO 10300-2 and ISO 10300-3 shall be valid only if the gear teeth are operated with a lubricant of proper viscosity and additive package for the load, speed and surface finish, and if there is a sufficient quantity of lubricant on the gear teeth and bearings to lubricate and maintain an acceptable operating temperature.

5.4.3 Misalignment

Many gear systems depend on external supports such as machinery foundations to maintain alignment of the gear mesh. If these supports are poorly designed, initially misaligned or become misaligned during operation due to elastic or thermal deflections or other influences, overall gear system performance will be adversely affected.

5.4.4 Deflection

Deflection of gear supporting housings, shafts and bearings due to external overhung, transverse and thrust loads affects tooth contact across the mesh. Since deflection varies with load, it is difficult to obtain good tooth contact at different loads. Generally, deflection due to external loads from driven and driving equipment reduces capacity, and this, as well as deflection caused by internal forces, should be taken into account when determining the actual gear tooth contact.

5.4.5 Materials and metallurgy

Most bevel gears are made from case-hardened steel. Allowable stress numbers for this and other materials shall be taken from gear tests, from special tests or, if the material is similar, from ISO 6336-5. Additionally, different modes of steel making and heat treatment are considered in ISO 6336-5. Hardness and tensile strength as well as the quality grade shall also be criteria for choosing permissible stress numbers.

NOTE Higher quality steel grades indicate higher allowable stress numbers, while lower quality grades indicate lower allowable stress numbers (see ISO 6336-5).

5.4.6 Residual stress

Any ferrous material having a case core relationship is likely to have residual stress. If properly managed, such stress will be compressive at the tooth surface, thereby enhancing the bending fatigue strength of the gear tooth. Shot peening, case carburizing and induction hardening, if properly performed, are common methods of inducing compressive pre-stress in the surface of the gear teeth. Improper grinding techniques after heat treatment can reduce the residual compressive stresses or even introduce residual tensile stresses in the root fillets of the teeth, thereby lowering the allowable stress numbers.

5.4.7 System dynamics

The method of analysis used in this document includes a dynamic factor, K_v , which derates the gears for increased loads caused by gear tooth inaccuracies. Generally speaking, this provides simplified values for easy application.

The dynamic response of the system results in additional gear tooth loads, due to the relative motions of the connected masses of the driver and the driven equipment. The application factor, K_A , is intended to account for the operating characteristics of the driving and driven equipment. It should be recognized, however, that if the operating roughness of the drive, gearbox or driven equipment causes excitation with a frequency that is near one of the system's major natural frequencies, resonant vibrations can cause severe overloads possibly several times higher than the nominal load. Therefore, where critical service applications are concerned, a vibration analysis of the complete system should be performed. This analysis shall comprise the total system, including driver, gearbox, driven equipment, couplings, mounting conditions and sources of excitation. Natural frequencies, mode shapes, and the dynamic response amplitudes should be calculated.

5.4.8 Contact pattern

The teeth of most bevel gears are crowned in both their profile and lengthwise directions during the manufacturing process in order to allow for deflection of the shafts and mountings. This crowning results in a localized contact pattern during roll testing under light loads. Under design load, unless otherwise specified, the tooth contact pattern is spread over the tooth flank without concentrations of the pattern at the edges of either gear member.

The application of the rating formulae to bevel gears manufactured under conditions in which this process has not been carried out and which do not have an adequate contact pattern, can require modifications of the factors given in this document. Such gears are not covered by ISO 10300 (all parts).

NOTE The total load used for contact pattern analysis can include the effects of an application factor (see [Annex D](#) for a fuller explanation of tooth contact development).

5.4.9 Corrosion

Corrosion of the gear tooth surface can have a significant detrimental effect on the bending strength and macropitting resistance of the teeth. However, the quantification of the effect of corrosion on gear teeth is beyond the range of ISO 10300 (all parts).

5.5 Further influence factors in the basic formulae

The basic formulae presented in ISO 10300-2 and ISO 10300-3 include factors reflecting gear geometry or being established by convention, which shall be calculated in accordance with their formulae.

In the formulae in ISO 10300 (all parts), there are also factors that reflect the effects of variations in manufacturing and service conditions of the unit. These are known as influence factors because they account for a number of influences. Although treated as independent, they can nevertheless affect each other to an extent that is beyond evaluation. They include the load factors, K_A , K_v , $K_{H\beta}$, $K_{F\beta}$, $K_{H\alpha}$ and $K_{F\alpha}$, as well as those factors influencing permissible stresses.

There are various methods of calculation to determine the influence factors. These are qualified, as needed, by the addition of subscripts A to C to the symbols. Unless otherwise specified (for example in an application standard), the more accurate method should be used for important transmissions. Supplementary subscripts should be used whenever the method used for evaluation of a factor would not otherwise be readily identifiable.

For some applications, it can be necessary to choose between factors determined by using alternative methods (for example, alternatives for the determination of the dynamic factor or the transverse

load factor). When reporting the calculation, the method used should be indicated by extending the subscript.

EXAMPLE $K_{v-C}, K_{H\alpha-B}$

6 External force and application factor, K_A

6.1 Nominal tangential force, torque, power

For the purposes of ISO 10300 (all parts), pinion torque is used in the basic stress calculation formulae. In order to determine the bending moment on the tooth, or the force on the tooth surface, the tangential force is calculated, at the reference cone at mid-facewidth, following [Formulae \(1\)](#) to [\(5\)](#):

Nominal tangential force of bevel gears, F_{mt} :

$$F_{mt1,2} = \frac{2000 \cdot T_{1,2}}{d_{m1,2}} \quad (1)$$

Nominal tangential force of virtual cylindrical gears, F_{vmt} :

$$F_{vmt} = F_{mt1} \cdot \frac{\cos \beta_v}{\cos \beta_{m1}} \quad (2)$$

Nominal torque of pinion and wheel, T :

$$T_{1,2} = \frac{F_{mt1,2} \cdot d_{m1,2}}{2000} = \frac{1000 \cdot P}{\omega_{1,2}} \approx \frac{9549 \cdot P}{n_{1,2}} \quad (3)$$

Nominal power, P :

$$P = \frac{F_{mt1,2} \cdot v_{mt1,2}}{1000} = \frac{T_{1,2} \cdot \omega_{1,2}}{1000} \approx \frac{T_{1,2} \cdot n_{1,2}}{9549} \quad (4)$$

Nominal tangential speed at mean point, v_{mt} :

$$v_{mt1,2} = \frac{d_{m1,2} \cdot \omega_{1,2}}{2000} \approx \frac{d_{m1,2} \cdot n_{1,2}}{19098} \quad (5)$$

6.2 Variable load conditions

If the load is not uniform, a careful analysis of the gear loads should be carried out, in which the external and internal factors are considered. All the different loads that occur during the anticipated life of the gears, and the duration of each load, should be determined. A method based on Miner's Rule (see ISO 6336-6) shall be used for determining the equivalent life of the gears for the torque spectrum.

6.3 Application factor, K_A

6.3.1 Application factor — General

In cases where no reliable experiences, or load spectra determined by practical measurement or comprehensive system analysis, are available, the calculation should use the nominal tangential force F_{mt} according to [6.1](#) and an application factor, K_A . This application factor makes allowance for any externally applied dynamic loads in excess of the nominal pinion torque, T_1 .

6.3.2 Influences affecting external dynamic loads

Many prime movers show peak loads. There are many possible sources of dynamic overload which should be considered, including:

- system vibration;
- critical speed;
- acceleration torques;
- overspeed;
- sudden variations in system operation;
- braking;
- negative torques, such as those produced by retarders on vehicles, which result in loading the reverse flanks of the gear teeth.

Analysis for critical speeds within the operating range of the drive train is essential. If critical speeds are present, changes in the design of the overall drive system shall be made in order to either eliminate them or provide system damping to minimize gear and shaft vibrations.

6.3.3 Establishment of application factors

Application factors are best established by a thorough analysis of service experience with a particular application. For applications such as marine gears, which are subjected to cyclic peak torques (torsional vibrations) and are designed for infinite life, the application factor can be defined as the ratio between cyclic peak torque and the nominal rated torque. The nominal rated torque is defined by the rated power and speed.

If the gear is subjected to a limited number of loads in excess of the amount of cyclic peak torque, this influence may be covered directly by means of cumulative fatigue analysis or by means of an increased application factor representing the influence of the load spectrum.

If service experience is unavailable, a thorough analytical investigation should be carried out. [Annex C](#) provides approximate values of K_A if neither of these alternatives is possible.

7 Dynamic factor, K_v

7.1 General

The dynamic factor, K_v , makes allowance for the effects of gear tooth quality related to speed and load as well as for the other parameters listed below (see [7.2](#) to [7.6](#)). The dynamic factor relates the total tooth load, including internal dynamic effects, to the transmitted tangential tooth load and is expressed as the sum of the internal effected dynamic load and the transmitted tangential tooth load, divided by the transmitted tangential tooth load. The parameters for the gear tooth internal dynamic load fall into two categories: design and manufacturing.

7.2 Design

The design parameters include:

- pitch line velocity;
- tooth load;
- inertia and stiffness of the rotating elements;

- tooth stiffness variation;
- lubricant properties;
- stiffness of bearings and case structure;
- critical speeds and internal vibration within the gear itself.

7.3 Manufacturing

The manufacturing parameters include:

- tooth spacing variations;
- runout of pitch surfaces with respect to the axis of rotation;
- tooth flank variations;
- compatibility of mating gear tooth elements;
- balance of parts;
- bearing fit and preload.

7.4 Transmission error

Even if the input torque and speed are constant, significant vibration of the gear masses and the resultant dynamic tooth forces can exist. These forces result from the relative displacements between the mating gears as they vibrate in response to an excitation known as transmission error. The ideal kinematics of a gear pair require a constant ratio between the input and output. Transmission error is defined as the deviation from uniform relative angular motion of the pair of meshing gears. It is influenced by all deviations from the ideal gear tooth form of the actual gear design, the manufacturing procedure and the operational conditions. The operational conditions include the following:

- Pitch line velocity: the frequencies of the excitation depend on the pitch line velocity and module.
- Gear mesh stiffness variations: as the gear teeth pass through the meshing cycle, gear mesh stiffness variations are a source of excitation especially pronounced in straight and Zerol bevel gears. Spiral bevel gears with a total contact ratio > 2 have less stiffness variation.
- Transmitted tooth load: since deflections are load dependent, gear tooth profile modifications can be designed to give uniform velocity ratio only for one load magnitude. Loads different from the design load increase the transmission error.
- Dynamic unbalance of the gears and shafts.
- Application environment: excessive wear and plastic deformation of the gear tooth profiles increase the transmission error. Gears shall have a properly designed lubrication system, enclosure, and seals to maintain a safe operating temperature and an environment free of contamination.
- Shaft alignment: gear tooth alignment is influenced by load and thermal deformations of gears, shafts, bearings and housings.
- Tooth friction induced excitation.

7.5 Dynamic response

The effects of dynamic tooth forces are influenced by the following:

- mass of the gears, shafts and other major internal components;
- stiffness of the gear teeth, gear blanks, shafts, bearings and housings;

- damping, of which the principal sources are the shaft bearings and seals, with other sources including the hysteresis of the gear shafts, viscous damping at sliding interfaces and couplings.

7.6 Resonance

7.6.1 General

When an excitation frequency (e.g. tooth meshing frequency, multiples of tooth meshing frequencies) coincides, or nearly coincides, with a natural frequency of the gearing system, a resonant vibration can cause high dynamic tooth loading. When the magnitude of internal dynamic load at such a driving speed becomes large, operation in this speed range should be avoided.

7.6.2 Gear blank resonance

The gearbox is just one component of a system comprising power source, gearbox, driven equipment and interconnecting shafts and couplings. The dynamic response of this system depends on its configuration. In certain cases, a system can possess a natural frequency close to the excitation frequency associated with an operating speed. Under such resonant conditions, its operation shall be carefully evaluated. For critical drives, a detailed analysis of the entire system should be performed. This should be taken into account when determining the effects on the application factor as these are external loads for the toothings.

7.7 Calculation methods for K_v

7.7.1 General comments

A bevel gear drive is a very complicated vibration system. The dynamic system as well as the natural frequencies which induce dynamic tooth loading cannot be determined by consideration of the pair of gears alone. The pinion shaft alignment can change considerably depending on the craftsmanship of the assembly, the backlash and the elastic deformation of gear shafts, bearings or housing.

A slight change in alignment alters the relative rotation angle of the gearing and thus the dynamic loading on the gears. Crowning in the lengthwise and profile directions can preclude true conjugate action and make tooth accuracy difficult to determine.

Under such circumstances, reliable values of the dynamic factor, K_v , can best be predicted by a mathematical model which has been satisfactorily verified by test measurements. If the known dynamic loads are added to the nominal transmitted load, then the dynamic factor should be set to unity.

To determine K_v , several methods are indicated in descending order of precision, from method A (K_{v-A}) to method C (K_{v-C}).

When using method B or C for hypoid gears which have a relative hypoid offset $a_{rel} > 0,1$, the dynamic factor is assumed to have the value 1 because of the damping properties of the sliding conditions in mesh.

NOTE This method is applicable to positive as well as to negative offset values. Only the absolute value of the offset is considered in [Formula \(7\)](#).

The dynamic factor, K_v , is calculated according to [Formula \(6\)](#):

$$K_v = K_v^* - \frac{K_v^* - 1}{0,1} \cdot a_{rel} \geq 1 \quad (6)$$

with $K_v^* = K_{v-B}$ according to [7.7.3](#) or $K_v^* = K_{v-C}$ according to [7.7.4](#);

$$a_{rel} = \frac{2 \cdot |a|}{d_{m2}} \quad (7)$$

7.7.2 Method A, K_{v-A}

K_{v-A} is determined by a comprehensive analysis, confirmed by experience of similar designs, using the following general procedures:

- a) a mathematical model of the vibration system is developed which refers to the entire power transmission, including the gearbox;
- b) the transmission error of the bevel gears under load is measured, or calculated by a reliable simulation programme for transmission error of bevel gears;
- c) the dynamic load response of the pinion and gear shafts is analysed with the system model, a), excited by the transmission error, b).

7.7.3 Method B, K_{v-B}

7.7.3.1 General

This method makes the simplifying assumption that the gear pair constitutes an elementary single mass and spring system comprising the combined masses of pinion and wheel, with a spring stiffness being the mesh stiffness of the contacting teeth. In accordance with this assumption, forces due to torsional vibrations of the shafts and coupled masses are not covered by K_{v-B} . This is realistic if other masses (apart from the gear pair) are connected by shafts of relatively low torsional stiffness. For bevel gears with significant lateral shaft flexibility, the real natural frequency will be less than calculated.

The amount of the dynamic overloads is, among other effects, a function of the accuracy of the gear, i.e. the flank form and pitch deviations. The flank form deviation of bevel gears is not as easy to measure as an involute form of cylindrical gears (see ISO/TR 10064-6^[2]), and ISO tolerances do not exist. However, single flank composite tolerances are specified in ISO 17485 and the transmission error of a bevel gear set should be checked accordingly if proper equipment is available. On the other hand, the pitch deviations can be measured relatively easily. So, in these cases, the simplifying assumption is made that the single pitch deviation is a representative value of the transmission error for determination of the dynamic factor.

The following data are needed for the calculation of K_{v-B} :

- a) accuracy of gear pair (single pitch deviation as specified in ISO 17485);
- b) mass moment of inertia of pinion and wheel (dimensions and material density);
- c) tooth stiffness;
- d) transmitted tangential load.

7.7.3.2 Speed ranges

The dimensionless reference speed is calculated according to [Formula \(8\)](#):

$$N = \frac{n_1}{n_{E1}} \tag{8}$$

where n_{E1} is the pinion resonance speed according to [7.7.3.3](#).

Because of the influence of stiffness values which are not included (for example those of shafts, bearings, housing), and because of the damping, the resonance speed can be above or below the speed calculated with [Formula \(9\)](#). For reasons of safety, a resonance sector of $0,75 < N \leq 1,25$ is defined.

This results in the following sectors for the calculation of K_{v-B} :

- subcritical sector, $N \leq 0,75$, determined by method A or B;

- main resonance sector, $0,75 < N \leq 1,25$, operation in this sector should be avoided, but if unavoidable, refined analysis by method A shall be carried out;
- intermediate sector, $1,25 < N < 1,5$, determined by method A or B;
- supercritical sector, $N \geq 1,5$, determined by method A or B.

See ISO 6336-1[1] for further information on the speed ranges.

7.7.3.3 Resonance speed

The resonance speed of pinion is derived by using [Formulae \(9\)](#) to [\(13\)](#):

$$n_{E1} = \frac{30 \cdot 10^3}{\pi \cdot z_1} \cdot \sqrt{\frac{c_\gamma}{m_{\text{red}}}} \quad (9)$$

where c_γ is the mean value of mesh stiffness [see [Formula \(11\)](#)];

$$m_{\text{red}} = \frac{m_1^* \cdot m_2^*}{m_1^* + m_2^*} \quad (10)$$

m_{red} is the mass per millimetre facewidth reduced to the line of action of the dynamically equivalent cylindrical gear pair.

A value of $c_{\gamma 0} = 20 \text{ N}/(\text{mm} \cdot \mu\text{m})$ applies to spur gears. Investigations of helical gears have shown that the stiffness decreases with increasing helix angles. On the other hand, the spiral arrangement of bevel gear teeth around a conical blank leads to higher rigidity of bevel gears, except straight bevel gears. Therefore, due to the lack of any better knowledge, the stiffness for a spur gear is assumed to be suitable for bevel gears in average conditions which are given by $F_{\text{vmt}} \cdot K_A / b_{\text{v,eff}} \geq 100 \text{ N/mm}$ and $b_{\text{v,eff}} / b_v \geq 0,85$.

The mean value of mesh stiffness per unit facewidth, c_γ , is determined by [Formula \(11\)](#):

$$c_\gamma = c_{\gamma 0} \cdot C_F \quad (11)$$

where

$c_{\gamma 0}$ is mesh stiffness for average conditions; a value of $20 \text{ N}/(\text{mm} \cdot \mu\text{m})$ should be used;

C_F is a correction factor of tooth stiffness for non-average conditions:

if $F_{\text{vmt}} \cdot K_A / b_{\text{v,eff}} \geq 100 \text{ N/mm}$:

$$C_F = 1 \quad (12)$$

if $F_{\text{vmt}} \cdot K_A / b_{\text{v,eff}} < 100 \text{ N/mm}$:

$$C_F = (F_{\text{vmt}} \cdot K_A / b_{\text{v,eff}}) / 100 \text{ N/mm} \quad (13)$$

$b_{\text{v,eff}}$ is the effective facewidth of the virtual cylindrical gear. The effective facewidth $b_{\text{v,eff}}$ is the real length of contact pattern (see [Annex D](#)). In the case of full load, the contact pattern typically has a minimum length of 85 % of facewidth b_v . If it is not possible to obtain information of contact pattern length under load conditions, $b_{\text{v,eff}} = 0,85 b_v$ should be used.

If an exact determination of the mass moments of inertia m_1^* and m_2^* of the bevel gears is either not feasible due to cost or otherwise impossible (for example, at the design stage), bevel gears of common

gear blank design should be replaced by approximate dynamically equivalent cylindrical gears (suffix x) (see [Figure 2](#)).

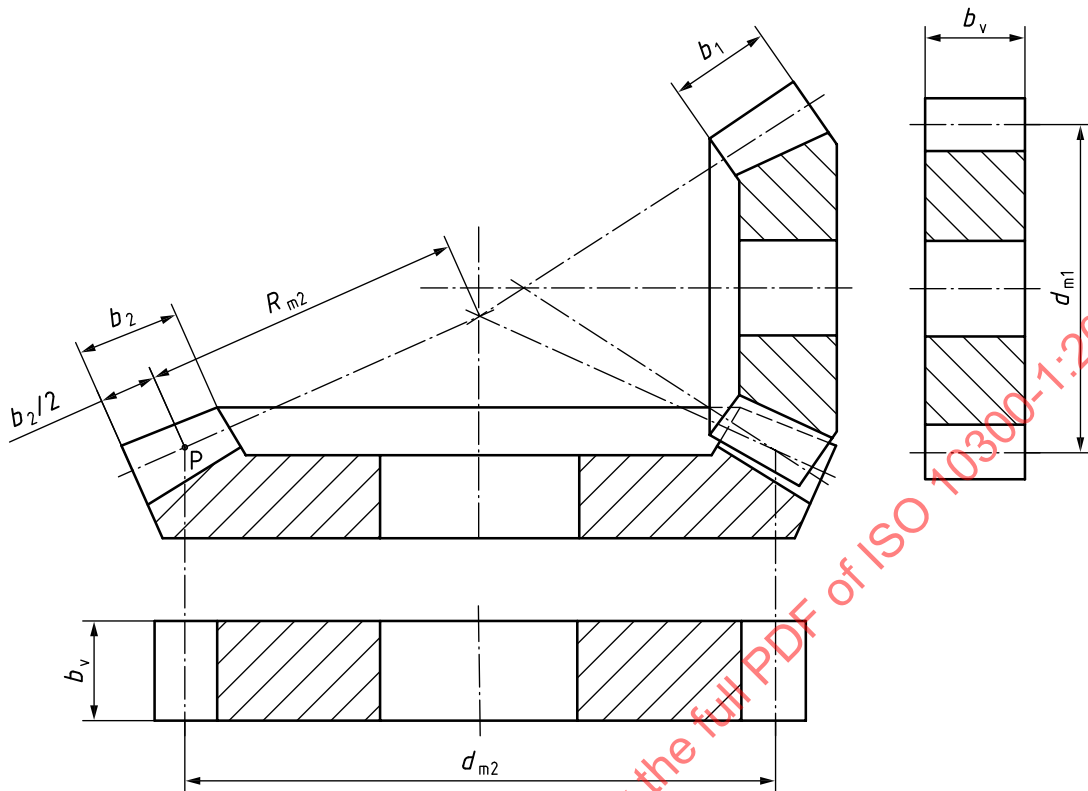


Figure 2 — Approximate dynamically equivalent cylindrical gears for the determination of the dynamic factor of bevel gears including hypoid gears

Relative gear mass per unit facewidth reduced to the line of action is calculated according to [Formula \(14\)](#):

$$m_{1,2}^* \approx m_{1x,2x}^* = \frac{1}{8} \cdot \rho \cdot \pi \cdot \frac{d_{m1,2}^2}{\cos^2[(\alpha_{nD} + \alpha_{nC})/2]} \quad (14)$$

where ρ is the density of the gear material (for steel $\rho = 7,86 \cdot 10^{-6} \text{ kg/mm}^3$).

7.7.3.4 Subcritical sector ($N \leq 0,75$)

Common operating range for industrial and vehicle gears:

$$K_{v-B} = N \cdot K + 1 \tag{15}$$

With the simplifying assumptions given in 7.7.3.1, Formula (16) applies:

$$K = \frac{b_v \cdot f_{p,eff} \cdot c'}{F_{vmt} \cdot K_A} \cdot c_{v1,2} + c_{v3} \tag{16}$$

where

$$f_{p,eff} = f_{pt} - y_p \text{ with } y_p \approx y_\alpha \tag{17}$$

See Formula (18) for c' ; Table 3 for $c_{v1,2}$ and c_{v3} ; see 9.3.1 for f_{pt} and 9.5 for y_α .

NOTE Any positive influence of tip relief or profile crowning is not considered. The calculation is, therefore, on the safe side for bevel gears which normally have profile crowning.

Table 3 — Influence factors c_{v1} to c_{v7} in Formulae (16) to (19) and (21)

| Influence factor | $1 < \varepsilon_{v\gamma} \leq 2^a$ | $\varepsilon_{v\gamma} > 2^a$ | — |
|------------------|--------------------------------------|--|--------------------------------|
| c_{v1}^b | 0,32 | 0,32 | } $c_{v1,2} = c_{v1} + c_{v2}$ |
| c_{v2}^c | 0,34 | $\frac{0,57}{\varepsilon_{v\gamma} - 0,3}$ | |
| c_{v3}^d | 0,23 | $\frac{0,096}{\varepsilon_{v\gamma} - 1,56}$ | |
| c_{v4}^e | 0,90 | $\frac{0,57 - 0,05 \cdot \varepsilon_{v\gamma}}{\varepsilon_{v\gamma} - 1,44}$ | |
| c_{v5}^f | 0,47 | 0,47 | } $c_{v5,6} = c_{v5} + c_{v6}$ |
| c_{v6}^f | 0,47 | $\frac{0,12}{\varepsilon_{v\gamma} - 1,74}$ | |
| — | $1 < \varepsilon_{v\gamma} \leq 1,5$ | $1,5 < \varepsilon_{v\gamma} \leq 2,5$ | $\varepsilon_{v\gamma} > 2,5$ |
| c_{v7}^g | 0,75 | $0,125 \cdot \sin[\pi(\varepsilon_{v\gamma} - 2)] + 0,875$ | 1,0 |

a For $\varepsilon_{v\gamma}$, see Formula (A.25) according to method B1 or Formula (B.25) according to method B2.
 b This influence factor allows for pitch deviation effects and is assumed to be constant.
 c This influence factor allows for tooth profile deviation effects.
 d This influence factor allows for the cyclic variation effect in mesh stiffness.
 e This influence factor takes into account resonant torsional oscillations of the gear pair, excited by cyclic variation of the mesh stiffness.
 f In the supercritical sector, the influences on K_{v-B} of the influence factors c_{v5} and c_{v6} correspond to those of c_{v1} and c_{v2} in the subcritical sector.
 g This influence factor takes into account the component of force which, due to mesh stiffness variation, is derived from tooth bending deflections during substantially constant speed.

A value of $c_0' = 14 \text{ N}/(\text{mm} \cdot \mu\text{m})$ applies to spur gears. Investigations of helical gears have shown that the tooth stiffness decreases with increasing helix angles. On the other hand, the spiral arrangement of bevel gear teeth around a conical blank leads to higher rigidity of bevel gears, except straight bevel gears. Therefore, due to the lack of any better knowledge, the tooth stiffness for a spur gear is assumed

to be suitable for bevel gears in average conditions which are given by $F_{vmt} \cdot K_A / b_{v,eff} \geq 100$ N/mm and $b_{v,eff} / b_v \geq 0,85$.

The single stiffness, c' , see ISO 6336-1,^[1] is determined as shown in [Formula \(18\)](#):

$$c' = c'_0 \cdot C_F \quad (18)$$

where

c'_0 is single stiffness for average conditions, a value of 14 N/(mm · μm) should be used;

C_F is a correction factor for non-average conditions [see [Formulae \(12\)](#) and [\(13\)](#)].

7.7.3.5 Main resonance sector ($0,75 < N \leq 1,25$)

With the simplifying assumptions given in [7.7.3.1](#), [Formula \(19\)](#) applies:

$$K_{v-B} = \frac{b_v \cdot f_{p,eff} \cdot c'}{F_{vmt} \cdot K_A} \cdot c_{v1,2} + c_{v4} + 1 \quad (19)$$

For $c_{v1,2}$ and c_{v4} see [Table 3](#).

7.7.3.6 Intermediate sector ($1,25 < N < 1,5$)

In the intermediate sector, the dynamic factor is determined by linear interpolation between K_{v-B} at $N = 1,25$ and K_{v-B} at $N = 1,5$. K_{v-B} is calculated according to [7.7.3.4](#) and [7.7.3.5](#), respectively according to [Formula \(20\)](#):

$$K_{v-B} = K_{v-B(N=1,5)} + \frac{K_{v-B(N=1,25)} - K_{v-B(N=1,5)}}{0,25} \cdot (1,5 - N) \quad (20)$$

7.7.3.7 Supercritical sector ($N \geq 1,5$)

High-speed gears and those with similar requirements operate in the supercritical sector, [Formula \(21\)](#) applies:

$$K_{v-B} = \frac{b_v \cdot f_{p,eff} \cdot c'}{F_{vmt} \cdot K_A} \cdot c_{v5,6} + c_{v7} + 1 \quad (21)$$

For c' and $f_{p,eff}$ see [7.7.3.3](#); for $c_{v5,6}$ and c_{v7} , see [Table 3](#).

7.7.4 Method C, K_{v-C}

7.7.4.1 General comments

The formulae for the calculation of the dynamic factor should be used in the absence of specific knowledge of the dynamic loads. [Formulae \(22\)](#) to [\(27\)](#) are based on empirical data, and do not account for resonance (see [7.6](#)).

Because of the approximate nature of the empirical formulation, and the lack of measured tolerance values at the design stage, the dynamic factor curve should be selected based on experience of manufacturing methods and taking into account the operating conditions affecting the design (see [7.7.1](#)). In most cases, the contact pattern on the tooth flank is helpful for comparison with previous experience.

The choice of the accuracy grade $B = 5$ to $B = 8$, which is considered in the empirical formulation of the dynamic factor, and “very accurate gearing” (see [7.7.4.2](#)), should be based on the transmission error (see

7.4). If transmission error is not available, it is reasonable to refer to the contact pattern on the tooth flank. If the contact pattern on each tooth flank is not uniform, pitch accuracy (single pitch deviation) can be incorporated as a representative value to determine the dynamic factor.

7.7.4.2 Very accurate gearing

Where gearing is manufactured using process control to very accurate gearing grades (generally speaking, when $B < 5$ in accordance with ISO 17485, or where design, manufacturing and application experience ensure a low transmission error), values of K_v between 1,0 and 1,1 may be used, depending on the specifier's experience with similar applications and the degree of accuracy actually achieved. In order to be able to use these values correctly, the gearing shall be maintained with accurate alignment and adequate lubrication so that its overall accuracy is maintained under the operating conditions.

7.7.4.3 Empirical curves

The following empirical formulae are generated with the following limitations for values of B , such that:

- $5 \leq B \leq 8$
- $6 \leq z \leq 1\,200$ or $(3\,000/m_{mn})$, whichever is less
- $1,25 \leq m_{mn} \leq 50$

Beyond the given maximum recommended wheel pitch line velocity $v_{et2,max}$ as shown in [Formula \(27\)](#), the given empirical formulations may be extrapolated based on experience and careful consideration of the factors influencing dynamic load.

The dynamic factor, K_{v-c} is calculated according to [Formulae \(22\) to \(26\)](#):

$$K_{v-c} = \left(\frac{A}{A + \sqrt{200 \cdot v_{et2}}} \right)^{-X} \quad (22)$$

where

$$v_{et2} = v_{mt2} \cdot \frac{d_{e2}}{d_{m2}} \quad (23)$$

$$A = 50 + 56 \cdot (1,0 - X) \quad (24)$$

$$X = 0,25 \cdot (B - 4,0)^{0,667} \quad (25)$$

B is the ISO accuracy grade as specified in ISO 17485, intended for the actual gear set.

The accuracy grade B may also be calculated with knowledge of the single pitch deviation:

$$B = 4 + 2,885\,39 \cdot \ln \left(\frac{f_{pt}}{0,003 \cdot d_T + 0,3 \cdot m_{mn} + 5} \right) \quad (26)$$

where

\ln is the natural logarithmic function, i.e. $\log_e()$;

d_T is the tolerance diameter according to ISO 17485;

m_{mn} is the mean normal module;

f_{pt} is the single pitch deviation (at mean point), in micrometres.

The maximum recommended pitch line velocity, $v_{et2,max}$, for a given accuracy grade B is determined as follows:

$$v_{et2,max} = \frac{[A+(13-B)]^2}{200} \quad (27)$$

where $v_{et2,max}$ is the maximum wheel pitch line velocity at the outer pitch diameter in metres per second.

8 Face load factors, $K_{H\beta}$, $K_{F\beta}$

8.1 General comments

The face load factors, $K_{H\beta}$ and $K_{F\beta}$, modify the rating formulae for the gear flank and for the tooth root to reflect the non-uniform distribution of the load along the facewidth.

$K_{H\beta}$ is defined as the ratio between the maximum load per unit facewidth and the mean load per unit facewidth.

$K_{F\beta}$ is defined as the ratio between the maximum tooth root stress and the mean tooth root stress along the facewidth.

The amount of non-uniform load distribution is influenced by:

- gear tooth manufacturing accuracy, and tooth contact pattern and spacing;
- alignment of the gears in their mountings;
- elastic deflections of the gear teeth, shafts, bearings, housings and foundations, which support the gear unit, resulting from either the internal or external gear loads;
- bearing clearances;
- Hertzian contact deformation of the tooth surfaces;
- thermal expansion and distortion of the gear unit due to operating temperatures (especially important on gear units where the gear housing is made from a different material than the gears, shafts and bearings);
- centrifugal deflections due to operating speeds.

The geometric characteristics of a bevel gear tooth change along its facewidth. Accordingly, the magnitudes of the axial and radial components of the tangential load vary with the position of the tooth contact. Similarly, the deflections of the mountings and of the tooth itself vary, and in turn affect the position of the tooth contact and its size and shape.

For applications in which the operating torque varies, the desired contact shall be considered “ideal” at full load only. For intermediate loads, a satisfactory compromise should be accepted.

This document is not applicable to bevel gears which have a poor contact pattern (see [5.4.8](#) and [Annex D](#)).

8.2 Method A

A comprehensive analysis of all influence factors, such as measurement of tooth root stress in service, is needed for an exact determination of the load distribution across the facewidth according to method A. However, due to its high cost, this type of analysis is generally restricted in practice.

8.3 Method B

A standardized approach for bevel gear face load factors corresponding to method B has not yet been developed. However, face load distribution can be determined on the basis of a loaded tooth contact analysis (LTCA).

8.4 Method C

8.4.1 Face load factor, $K_{H\beta-C}$

In the case of bevel gears, the face load distribution is influenced essentially by the crowning of the gear teeth and by the deflections occurring in service. This is considered in the calculation of the length of the contact line (see [Annex A](#)) as well as in the calculation of the load distribution (see ISO 10300-2:2023, Figure 2), which applies, however, only to gear sets with satisfactory contact patterns as defined in [Annex D](#).

The influence of the deflections, and thus of the bearing arrangement, is accounted for by the mounting factor, $K_{H\beta-be}$, according to [Table 4](#).

The face load factor, $K_{H\beta-C}$, is calculated according to [Formula \(28\)](#):

$$K_{H\beta-C} = 1,5 \cdot K_{H\beta-be} \quad (28)$$

NOTE [Formula \(28\)](#) is not valid for uncrowned gears.

Table 4 — Mounting factor, $K_{H\beta-be}$

| Verification of contact pattern | Mounting conditions of pinion and wheel | | |
|---|---|-------------------------------|---------------------------------|
| | Neither member cantilever mounted | One member cantilever mounted | Both members cantilever mounted |
| for each gear set in its housing under full load | 1,00 | 1,00 | 1,00 |
| for each gear set under light test load | 1,05 | 1,10 | 1,25 |
| for a sample gear set and estimated for full load | 1,20 | 1,32 | 1,50 |

NOTE Based on optimum tooth contact as evidenced by results of a contact pattern test on the gears in their mountings.

The observed contact pattern is normally an accumulated picture of each possible tooth pair combination. [Formula \(28\)](#) is valid only if the movement of the tooth contact pattern, during one revolution of the wheel, either towards the heel or toe, is small. Otherwise, the smallest contact pattern should be taken for the determination of $b_{v,eff}$. This movement of single contact patterns can be particularly pronounced for gears finished by lapping only.

8.4.2 Local face load factor, $K_{H\beta,Y}$

For the localized calculation methods according to ISO/TS 10300-20 and ISO 10300-2:2023, Annex A, the local face load factor, $K_{H\beta,Y}$, for contact stress shall be calculated with [Formulae \(29\)](#) to [\(31\)](#).

$$K_{H\beta,Y} = K_{H\beta} \cdot \left[1 - (b_Y \cdot z_Y)^a \right] \quad (29)$$

with auxiliary values

$$z_Y = \sqrt{\left(\frac{b_{v,eff}}{2} - \frac{x_{1,Y} + x_{2,Y}}{2} \right)^2 + \left(g_{va2} - \frac{g_{v\alpha}}{2} + g_Y - \frac{y_{1,Y} + y_{2,Y}}{2} \right)^2} \quad (30)$$

$$a = \frac{1}{K_{H\beta} - 1}; \quad b_Y = \frac{2}{l_{b,Y}} \quad (31)$$

where $K_{H\beta}$ is the face load factor.

The local geometry data shall be calculated according to the given calculation method in [Annex A](#).

8.4.3 Face load factor, $K_{F\beta-C}$

$K_{F\beta-C}$ accounts for the effect of the load distribution across the facewidth on the tooth root stress and is calculated according to [Formula \(32\)](#):

$$K_{F\beta-C} = K_{H\beta-C} / K_{F0} \quad (32)$$

For $K_{H\beta}$ see [8.4.1](#); K_{F0} see [8.4.4](#).

8.4.4 Lengthwise curvature factor for bending strength, K_{F0}

The lengthwise curvature factor, K_{F0} , considers the contact pattern shift under different loads which is smallest, if the lengthwise tooth curvature at the mean point corresponds to that of an involute curve. This effect is well known and depends on the cutter radius r_{c0} and the spiral angle β_{m2} .

The following two cases shall be considered.

- a) For straight and Zerol bevel gears as well as spiral bevel gears with large cutter radii ($r_{c0} > R_{m2}$), [Formula \(33\)](#) applies:

$$K_{F0} = 1,0 \quad (33)$$

- b) For other spiral bevel and hypoid gears, [Formula \(34\)](#) applies:

$$K_{F0} = 0,211 \cdot \left(\frac{\rho_{m\beta}}{R_{m2}} \right)^q + 0,789 \quad (34)$$

where

$\rho_{m\beta}$ is the lengthwise tooth mean radius of curvature;

R_{m2} is mean cone distance of the wheel.

$$q = \frac{0,279}{\lg(\sin \beta_{m2})} \quad (35)$$

The lengthwise tooth mean radius of curvature, $\rho_{m\beta}$, (see ISO 23509) is calculated using [Formula \(36\)](#) to [\(39\)](#):

- for face milled gears:

$$\rho_{m\beta} = r_{c0} \quad (36)$$

- for face hobbled gears:

$$\rho_{m\beta} = R_{m2} \cdot \cos \beta_{m2} \cdot \left[\tan \beta_{m2} + \frac{\tan \eta_1}{1 + \tan \nu_0 \cdot (\tan \beta_{m2} + \tan \eta_1)} \right] \quad (37)$$

where

$$v_0 = \arcsin\left(\frac{m_{mn} \cdot z_0}{2 \cdot r_{c0}}\right) \quad (38)$$

$$\eta_1 = \arccos\left[\frac{R_{m2} \cdot \cos \beta_{m2}}{\sqrt{R_{m2}^2 + r_{c0}^2 - 2 \cdot R_{m2} \cdot r_{c0} \cdot \sin(\beta_{m2} - v_0)}} \cdot \left(1 + \frac{z_0}{z_2} \cdot \sin \delta_2\right)\right] \quad (39)$$

The range of validity of face load factor, K_{F0} , is limited.

If the calculated value of $K_{F0} > 1,15$ set $K_{F0} = 1,15$; if the calculated value of $K_{F0} < 1,00$ set $K_{F0} = 1,0$.

9 Transverse load factors, $K_{H\alpha}$, $K_{F\alpha}$

9.1 General comments

The distribution of the total tangential force over several pairs of meshing teeth depends, in the case of given gear dimensions, on the gear accuracy and the amount of the total tangential force.

The factor $K_{H\alpha}$ accounts for the effect of the load distribution on the contact stress, while $K_{F\alpha}$ accounts for the effect of the load distribution on the tooth root stress (see ISO 6336-1^[1] for further information). The use of method A requires comprehensive analysis (see 9.2), whereas the methods of approximation B and C (see 9.3 and 9.4) are sufficiently accurate in most cases.

When using methods B or C, the transverse load factors for gears with small offset are interpolated between the value for non-offset bevel gears and 1. The value 1 is assumed to be a realistic value for hypoid gears with a typical amount of offset (see 7.1) because the running-in effect adapts the flanks under load.

For method B, $K_{H\alpha}^*$ or $K_{F\alpha}^*$ shall be calculated according to 9.3.

For method C, $K_{H\alpha}^*$ or $K_{F\alpha}^*$ shall be derived from Table 5.

Transverse load factors, $K_{H\alpha}$, $K_{F\alpha}$ shall be calculated according to Formulae (40) and (41):

$$K_{H\alpha} = K_{F\alpha} = K_{H\alpha}^* \frac{K_{H\alpha}^* - 1}{0,1} \cdot a_{rel} \geq 1 \quad (40)$$

NOTE If $K_{H\alpha}/K_{F\alpha} < 1$ then $K_{H\alpha}/K_{F\alpha}$ are set to 1.

with $K_{H\alpha}^* = K_{H\alpha-B}^*$ according to 9.3 or $K_{H\alpha}^* = K_{H\alpha-C}^*$ according to 9.4;

$$a_{rel} = \frac{2 \cdot |a|}{d_{m2}} \quad (41)$$

When using method B for the calculation of the transverse load factors (see 9.3), the following boundary conditions shall be considered:

For method B1, Formulae (42) and (43) apply:

$$1 \leq K_{H\alpha} \leq \varepsilon_{v\gamma} / (\varepsilon_{v\alpha} \cdot Z_{LS}^2) \quad (42)$$

$$1 \leq K_{F\alpha} \leq \varepsilon_{v\gamma} / (\varepsilon_{v\alpha} \cdot Y_{LS}) \quad (43)$$

with Z_{LS} and Y_{LS} as specified in 6.4.2 of ISO 10300-2:2023 and 6.4.5 of ISO 10300-3:2023.

For method B2, [Formulae \(44\)](#) and [\(45\)](#) apply:

$$1 \leq K_{H\alpha} \leq \varepsilon_{v\gamma} / (\varepsilon_{v\alpha} \cdot \varepsilon_{NI}) \quad (44)$$

$$1 \leq K_{F\alpha} \leq \varepsilon_{v\gamma} / (\varepsilon_{v\alpha} \cdot \varepsilon_N) \quad (45)$$

with ε_{NI} and ε_N as specified in 7.4.2.3 of ISO 10300-2:2023 and 7.4.4.3 and 7.4.5.2 of ISO 10300-3:2023.

If the calculated value $K_{H\alpha}$ or rather $K_{F\alpha}$ exceeds one of both limits, $K_{H\alpha}$ or rather $K_{F\alpha}$ is set to the respective limit value.

With these boundary conditions, the most unfavourable load distribution is assumed, i.e. only one pair of teeth transmits the total tangential force, and the calculation is therefore on the safe side. The accuracy of bevel gears should be chosen so that neither $K_{H\alpha}$ nor $K_{F\alpha}$ exceeds the value of $\varepsilon_{v\alpha n}$.

9.2 Method A

The load distribution taken as the basis for the load capacity calculation should be determined by measurement or by an exact analysis of all influence factors. However, when the latter is used, the method's accuracy and reliability shall be proved, and its premises clearly presented.

9.3 Method B

9.3.1 Bevel gears having virtual cylindrical gears with contact ratio $\varepsilon_{v\gamma} \leq 2$

Transverse load factors, $K_{H\alpha-B}^*$, $K_{F\alpha-B}^*$ shall be calculated according to [Formulae \(46\)](#) and [\(47\)](#):

$$K_{H\alpha-B}^* = K_{F\alpha-B}^* = \frac{\varepsilon_{v\gamma}}{2} \cdot \left[0,9 + 0,4 \cdot \frac{c_\gamma \cdot (f_{pt} - y_\alpha)}{F_{mtH} / b_v} \right] \quad (46)$$

where

c_γ is the mesh stiffness, as an approximation, $c_\gamma = 20 \text{ N}/(\text{mm} \cdot \mu\text{m})$ (see [7.7.3.3](#));

f_{pt} is the single pitch deviation, maximum value of pinion or wheel; for design calculations, the tolerance of the wheel according to ISO 17485 should be used;

y_α is the running-in allowance (see [9.5](#));

F_{mtH} is the determinant tangential force at mid-facewidth on the pitch cone.

$$F_{mtH} = F_{vmt} \cdot K_A \cdot K_V \cdot K_{H\beta} \quad (47)$$

9.3.2 Bevel gears having virtual cylindrical gears with contact ratio $\varepsilon_{v\gamma} > 2$

Transverse load factors, $K_{H\alpha-B}^*$, $K_{F\alpha-B}^*$ shall be calculated according to [Formula \(48\)](#):

$$K_{H\alpha-B}^* = K_{F\alpha-B}^* = 0,9 + 0,4 \cdot \sqrt{\frac{2 \cdot (\varepsilon_{v\gamma} - 1)}{\varepsilon_{v\gamma}}} \cdot \frac{c_\gamma \cdot (f_{pt} - y_\alpha)}{F_{mtH} / b_v} \quad (48)$$

for c_γ , f_{pt} , y_α , F_{mtH} see [9.3.1](#).

9.4 Method C

9.4.1 General comments

Method C is, in general, sufficiently accurate for industrial gears. To determine the transverse load factors $K_{H\alpha-C}^*$, $K_{F\alpha-C}^*$, the gear accuracy grade, specific loading, gear type and running-in behaviour are required. The running-in behaviour is expressed by material and type of heat treatment.

9.4.2 Assumptions

The following assumptions are valid for method C:

- a transverse contact ratio of $1,2 < \epsilon_{v\alpha} < 1,9$ applies to tooth stiffness (see ISO 6336-1[1]);
- stiffness values of $c_\gamma = 20 \text{ N}/(\text{mm} \cdot \mu\text{m})$ according to Formula (11) or $c' = 14 \text{ N}/(\text{mm} \cdot \mu\text{m})$ according to Formula (18);
- a single pitch deviation is assigned to each gear accuracy grade. With this assumption, transverse load distribution factors are obtained which are on the safe side for most applications, i.e. in case of mean and high specific loadings, as well as in case of specific loadings $F_{vmt} \cdot K_A / b_{v,eff} < 100 \text{ N}/\text{mm}$.

9.4.3 Determination of the factors

$K_{H\alpha-C}^*$ and $K_{F\alpha-C}^*$ shall be taken from Table 5.

If the gear accuracy grades are different for pinion and wheel, the worse one shall be used.

Table 5 — Transverse load distribution factors, $K_{H\alpha-C}^*$ and $K_{F\alpha-C}^*$

| Specific loading $F_{vmt} \cdot K_A / b_{v,eff}$ | | | $\geq 100 \text{ N}/\text{mm}^2$ | | | | | | $< 100 \text{ N}/\text{mm}^2$ | |
|---|--------------------------------|-------------------|----------------------------------|-----|-----|-----|---|--|-------------------------------|--------------------------|
| Gear accuracy grade (see 5.3.2) | | | 5 and better | 6 | 7 | 8 | 9 | 10 | 11 | All accuracy grades |
| Surface hardened | Straight bevel gears | $K_{H\alpha-C}^*$ | 1,0 | 1,1 | 1,2 | | | (B1): $1 / Z_{LS}^2$ or 1,2 | | Whichever is the greater |
| | | $K_{F\alpha-C}^*$ | | | | | | (B2): $1 / \epsilon_{NI}$ or 1,2 | | Whichever is the greater |
| | Helical and spiral bevel gears | $K_{H\alpha-C}^*$ | 1,0 | 1,1 | 1,2 | 1,4 | | $\epsilon_{v\alpha n}$ or 1,4 whichever is the greater | | |
| | | $K_{F\alpha-C}^*$ | | | | | | | | |
| Not surface hardened | Straight bevel gears | $K_{H\alpha-C}^*$ | 1,0 | | 1,1 | 1,2 | | (B1): $1 / Z_{LS}^2$ or 1,2 | | Whichever is the greater |
| | | $K_{F\alpha-C}^*$ | | | | | | (B2): $1 / \epsilon_{NI}$ or 1,2 | | Whichever is the greater |
| | Helical and spiral bevel gears | $K_{H\alpha-C}^*$ | 1,0 | 1,1 | 1,2 | 1,4 | | $\epsilon_{v\alpha n}$ or 1,4 whichever is the greater | | |
| | | $K_{F\alpha-C}^*$ | | | | | | | | |

NOTE For Z_{LS} , ϵ_{NI} and Y_{LS} , ϵ_N see 9.1. (B1) and (B2) stands for method B1 and method B2.

9.5 Running-in allowance, y_α

The running-in allowance, y_α , is the amount due to running-in by which the mesh alignment error is reduced from the start of the operation.

The running in allowance, y_{α} , can be calculated using [Formulae \(49\)](#) to [\(52\)](#) (where f_{pt} is single pitch deviation, see [9.3.1](#)).

For through hardened steels:

$$y_{\alpha} = \frac{160}{\sigma_{H,lim}} \cdot f_{pt} \tag{49}$$

for $v_{mt2} \leq 5$ m/s: without restriction;

for $5 \text{ m/s} < v_{mt2} \leq 10$ m/s: $y_{\alpha} \leq 12\,800/\sigma_{H,lim}$;

for $v_{mt2} > 10$ m/s: $y_{\alpha} \leq 6\,400/\sigma_{H,lim}$.

For grey cast iron:

$$y_{\alpha} = 0,275 \cdot f_{pt} \tag{50}$$

for $v_{mt2} \leq 5$ m/s: without restriction;

for $5 \text{ m/s} < v_{mt2} \leq 10$ m/s: $y_{\alpha} \leq 22 \mu\text{m}$;

for $v_{mt2} > 10$ m/s: $y_{\alpha} \leq 11 \mu\text{m}$.

For case hardened and nitrided gears:

$$y_{\alpha} = 0,075 \cdot f_{pt} \tag{51}$$

for all speeds with the restriction: $y_{\alpha} \leq 3 \mu\text{m}$.

If materials of pinion and wheel are different, a mean value for y_{α} shall be calculated:

$$y_{\alpha} = \frac{y_{\alpha 1} + y_{\alpha 2}}{2} \tag{52}$$

wherein $y_{\alpha 1}$ shall be determined for the pinion material and $y_{\alpha 2}$ for the wheel material.

Annex A (normative)

Calculation of virtual cylindrical gears — Method B1

A.1 General

Approved rating procedures for macropitting resistance and bending strength of bevel and hypoid gears which can serve as a standard are based on virtual cylindrical gears. The main reason is that the necessary allowable stress values can be taken from tests of cylindrical gears which are easier to get and statistically more reliable than those from the fewer tests of bevel or hypoid gears.

The decisive requirement for this approach is a good equivalence between the meshing conditions of bevel or hypoid gears and of their corresponding virtual cylindrical gears. In order to ensure this, exact tooth contact analysis calculations (TCA) were carried out for a broad variety of bevel and hypoid gears and compared with the meshing conditions of the corresponding virtual cylindrical gears. By this means, the known formulae for bevel gears without offset were confirmed and new extended formulae including hypoid gears were defined. The latter refers to major parameters of virtual cylindrical gears, such as helix angle, facewidth, contact ratio, radius of relative curvature.

Besides, the virtual cylindrical gears for hypoids were developed such that with decreasing offset values, they continuously approximate to the known dimensions of those for spiral bevel gears without offset. The advantage is that also the calculated load capacities of these hypoid gears approximate to the proven good results of spiral bevel gears.

So, [Annex A](#) contains geometric relations for generating the data of the required virtual cylindrical gears. The gear data presented here apply exclusively to gears with $(x_{hm1} + x_{hm2}) = 0$. The initial bevel or hypoid gear data necessary for these calculations should conform to ISO 23509.

Calculations shall be carried out for pinion and wheel together; however, in case of different pressure angles of drive and coast side (hypoid gears, asymmetric bevel gears) separately for drive and coast side flank.

A.2 Data of virtual cylindrical gears in transverse section (suffix v)

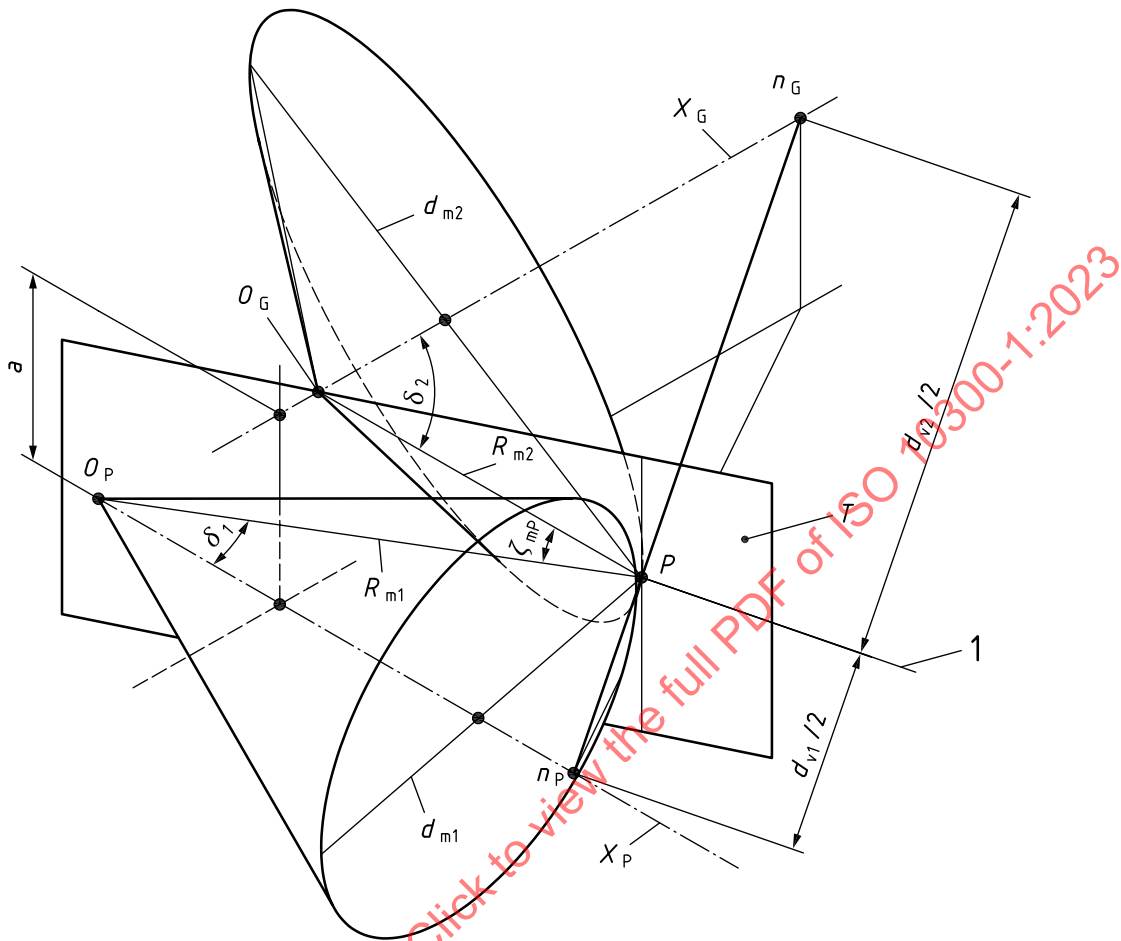
A.2.1 General

If a transverse section of a bevel gear tooth at midface is developed into the sectional plane, a virtual cylindrical gear is obtained with nearly involute teeth. This is standard practice for bevel gears without hypoid offset (see [Figure A.2](#)). For hypoid gears which are geometrically the most general type of gearing, a similar procedure is applicable. Looking at [Figure A.1](#), a schematic diagram of hypoid gears (see also ISO 23509:2016, [Figure A.2](#)) shows a common tangential plane T between both pitch cones with diameters d_{m1} and d_{m2} , which contact each other at the mean point P . Besides, both pitch cones contact with the tangential plane T along lines which are designated as mean cone distances R_{m1} and R_{m2} and include the offset angle ζ_{mp} .

A normal line to the plane T , erected in the mean point, intersects with the pinion axis at n_p and with the wheel axis at n_G . This line corresponds to line Q of [Figure A.2](#) representing the centre distance a_v of virtual cylindrical gears. With hypoid gears, however, the pinion axis and wheel axis are not in the same plane. In order to get virtual cylindrical gears with parallel axes, an approximation is made by giving both axes the direction, which divides the offset angle ζ_{mp} into half.

It is not assumed that thus-defined virtual cylindrical gears have the same meshing conditions as hypoid gears. This is adjusted afterwards by several appropriate correction factors such as the hypoid

factor Z_{Hyp} which accounts for the influence of the lengthwise sliding of hypoid gear teeth. However, virtual cylindrical gears supply the required geometrical basis to achieve a practicable rating system for all types of bevel gears.



Key

- 1 bisecting line of the offset angle ζ_{mp}

Figure A.1 — Schematic diagram of hypoid gear

A.2.2 Determination of the diameters, d_v

For the determination of the diameters, d_v , [Formulae \(A.1\)](#) to [\(A.7\)](#) apply.

Reference diameter, d_v :

$$d_{v1,2} = \frac{d_{m1,2}}{\cos \delta_{1,2}} \tag{A.1}$$

for hypoid gears:

$$d_{m2} \neq u \cdot d_{m1} \tag{A.2}$$

for $a = 0$ and $\Sigma = 90^\circ$:

$$d_{v1} = d_{m1} \cdot \frac{\sqrt{u^2 + 1}}{u} \tag{A.3}$$

$$d_{v2} = u^2 \cdot d_{v1} \tag{A.4}$$

Centre distance, a_v :

$$a_v = (d_{v1} + d_{v2}) / 2 \tag{A.5}$$

Tip diameter, d_{va} :

$$d_{va1,2} = d_{v1,2} + 2 \cdot h_{am1,2} \tag{A.6}$$

Root diameter, d_{vf} :

$$d_{vf1,2} = d_{v1,2} - 2 \cdot h_{fm1,2} \tag{A.7}$$

From [Figure A.1](#), it is also conceivable that the hypoid offset, a , and simultaneously the offset angle, ζ_{mp} , decrease until at $a = 0$ the special case of bevel gears without offset is reached and the cone distances R_{m1} and R_{m2} coincide. Then, the well-known former parameters of virtual cylindrical gears are valid again as given in [Figure A.2](#).

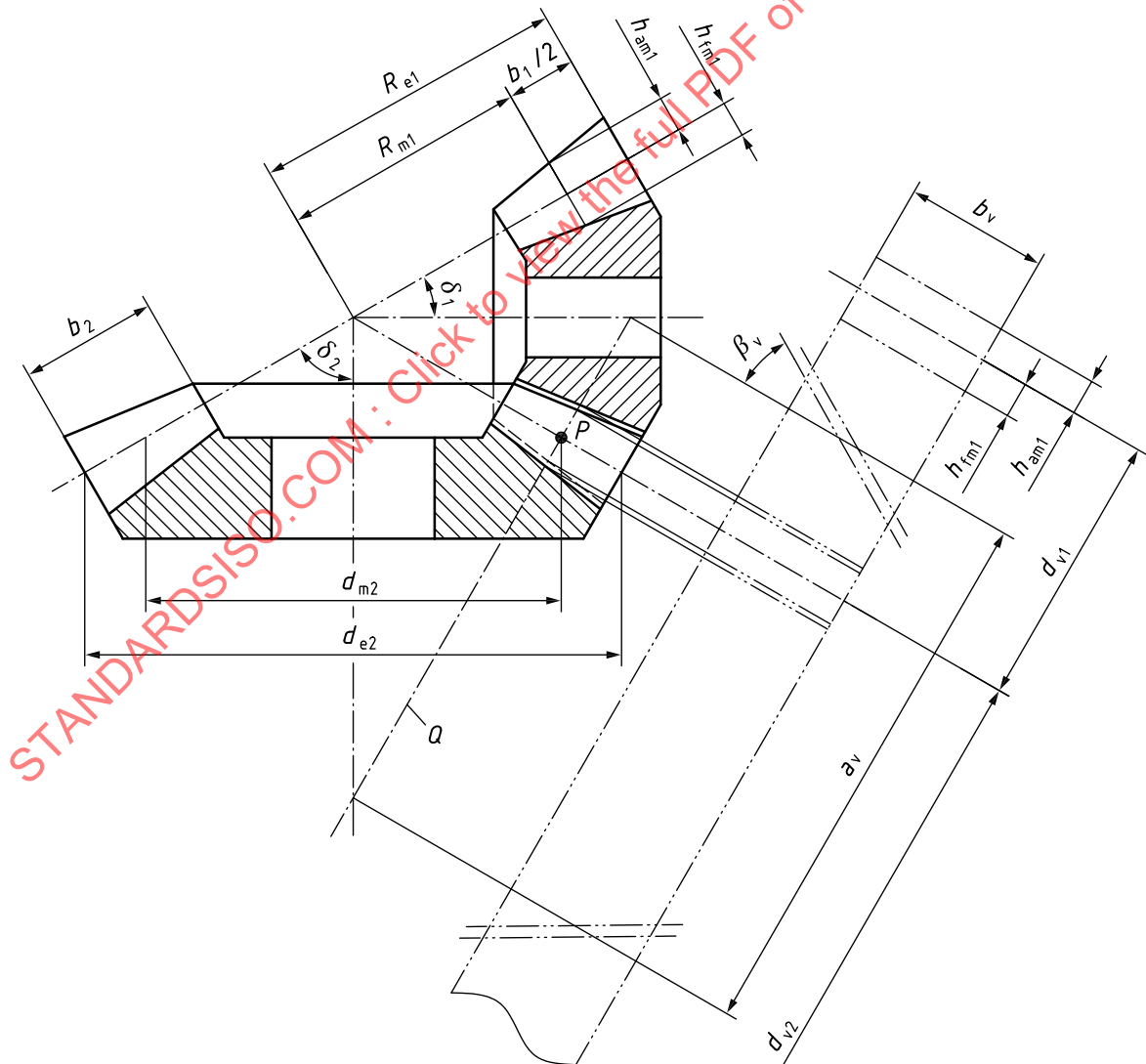


Figure A.2 — Bevel gears without offset and their corresponding virtual cylindrical gears

A.2.3 Determination of the helix angle, β_v

For bevel gears without offset, the helix angle β_v of virtual cylindrical gears is equal to the spiral angle of the pinion β_{m1} and the wheel β_{m2} because $\beta_{m1} = \beta_{m2}$. However, this is not true with hypoid gears where $\beta_{m1} = \beta_{m2} + \zeta_{mp}$ (see ISO 23509). In order to find the one helix angle for the virtual cylindrical gear pair, it is referred to [Figure A.1](#) where the bisecting line of the angle ζ_{mp} defines the direction of the virtual pinion axis and wheel axis. Then, the pinion helix angle is $\beta_{m1} - \zeta_{mp}/2$, is equal to the wheel helix angle $\beta_{m2} + \zeta_{mp}/2$, and both are equal to the helix angle β_v of the virtual cylindrical gear pair.

On this basis a comparison of the meshing conditions mentioned in [Clause A.1](#) was applied. The inclination angle β_B between the contact line and the pitch line in the mean point was used as a representative parameter in this case. It turned out that the inclination angle β_B calculated by TCA for any bevel or hypoid gear has nearly the same value as calculated for the corresponding virtual cylindrical gear with helix angle β_v which is the arithmetic mean value of both spiral angles β_{m1} and β_{m2} .

NOTE In this context, contact line means the major axis of the Hertzian contact ellipse under load.

The helix angle and further parameters of the virtual cylindrical gears shall be calculated according to [Formulae \(A.8\)](#) to [\(A.18\)](#).

Helix angle, β_v :

$$\beta_v = \frac{\beta_{m1} + \beta_{m2}}{2} \tag{A.8}$$

Base diameter, d_{vb} :

$$d_{vb1,2} = d_{v1,2} \cdot \cos \alpha_{vet} \tag{A.9}$$

where

$$\alpha_{vet} = \arctan(\tan \alpha_e / \cos \beta_v) \tag{A.10}$$

a) $\alpha_e = \alpha_{eD}$ for drive side (see ISO 23509);

b) $\alpha_e = \alpha_{eC}$ for coast side (see ISO 23509)

Transverse module, m_{vt} :

$$m_{vt} = m_{mn} / \cos \beta_v \tag{A.11}$$

Number of teeth, z_v :

$$z_{v1,2} = d_{v1,2} / m_{vt} \tag{A.12}$$

Gear ratio, u_v :

$$u_v = z_{v2} / z_{v1} \tag{A.13}$$

$$\text{for } a = 0 \text{ and } \Sigma = 90^\circ: z_{v1} = z_1 \cdot \frac{\sqrt{u^2 + 1}}{u} \tag{A.14}$$

$$z_{v2} = z_2 \cdot \sqrt{u^2 + 1} \quad (\text{A.15})$$

Helix angle at base circle, β_{vb} :

$$\beta_{vb} = \arcsin(\sin \beta_v \cdot \cos \alpha_e) \quad (\text{A.16})$$

where

$\alpha_e = \alpha_{eD}$ for drive side (see ISO 23509);

$\alpha_e = \alpha_{eC}$ for coast side (see ISO 23509).

Transverse base pitch, p_{vet} :

$$p_{vet} = \pi \cdot m_{mn} \cdot \cos \alpha_{vet} / \cos \beta_v \quad (\text{A.17})$$

Length of path of contact, $g_{v\alpha}$:

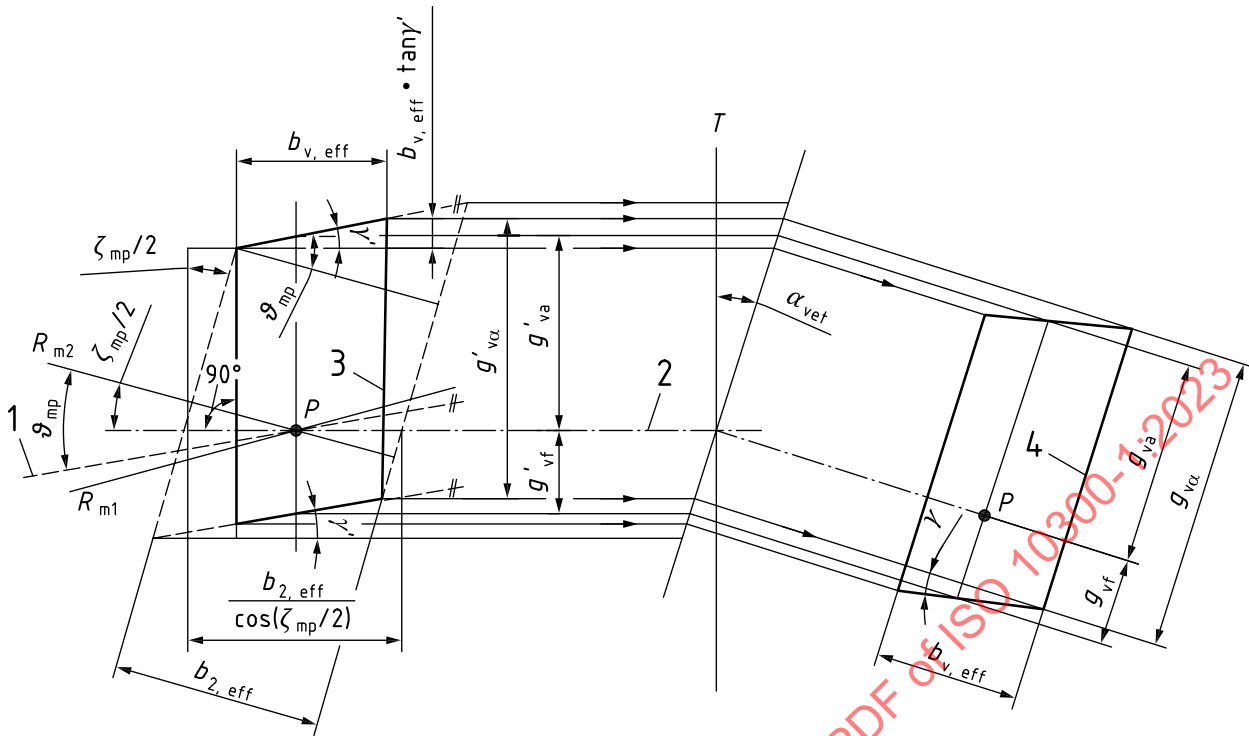
$$g_{v\alpha} = \frac{1}{2} \cdot \left[\left(\sqrt{d_{va1}^2 - d_{vb1}^2} - d_{v1} \cdot \sin \alpha_{vet} \right) + \left(\sqrt{d_{va2}^2 - d_{vb2}^2} - d_{v2} \cdot \sin \alpha_{vet} \right) \right] \quad (\text{A.18})$$

A.2.4 Determination of the facewidth, b_v

Whereas the facewidth of virtual cylindrical gears and of their corresponding bevel gears without offset have the same size ($b_v = b$, see [Figure A.2](#)), this is not true for hypoid gears. Before the facewidth b_v is calculated, the effective facewidth $b_{v,eff}$ of the virtual cylindrical gear pair shall be determined. For that purpose, the length of the contact pattern $b_{2,eff}$ which is measured in the direction of the wheel facewidth, is used.

Simplified, it is assumed that the theoretical zone of action of the hypoid wheel is not arched but developed into a parallelogram and then projected on to the common pitch plane T as shown in [Figure A.3](#) by dotted bold lines. The side lines of this zone of action around mean point P are vertical to the wheel axis which in this view coincides with the cone distance R_{m2} . The other two boundary lines are parallel to the instantaneous axis of helical relative motion of the hypoid gear pair which is given by the angle ϑ_{mp} .

The zone of action of the corresponding virtual cylindrical gear pair is the greatest possible parallelogram (bold lines in [Figure A.3](#)) inscribed in the theoretical zone of action of the wheel whereby the side lines now are vertical to the axis of roll of the virtual cylindrical gear pair given by the angle $\zeta_{mp}/2$. The width of this smaller parallelogram appears in the given view in true length and it is the effective facewidth $b_{v,eff}$ of the virtual cylindrical gear pair. To get the complete zone of action in true size, the given top view is projected into the plane inclined by the effective pressure angle, α_{vet} , of the active flank in which the path of contact is also in true size (see key item 4 of [Figure A.3](#)).



Key

- 1 axis of relative helical motion of the hypoid gears
- 2 axis of roll of the virtual cylindrical gears
- 3 projected zone of action in tangential plane (dimensions of bevel gears)
- 4 zone of action in meshing plane (dimensions of virtual cylindrical gears)

Figure A.3 — Simplified zone of action for virtual cylindrical gears

Formula (A.19) is derived from Figure A.3:

Effective facewidth, $b_{v,eff}$:

$$b_{v,eff} = \frac{(b_{2,eff} / \cos(\zeta_{mp} / 2) - g_{v\alpha} \cdot \cos \alpha_{vet} \cdot \tan(\zeta_{mp} / 2))}{1 - \tan \gamma' \cdot \tan(\zeta_{mp} / 2)} \tag{A.19}$$

where

$$\gamma' = \vartheta_{mp} - \zeta_{mp} / 2 \tag{A.20}$$

$$\vartheta_{mp} = \arctan(\sin \delta_2 \cdot \tan \zeta_m) \tag{A.21}$$

α_{vet} is the effective pressure angle of the virtual cylindrical gears calculated for the active flank, see Formula (A.10);

for ζ_{mp} and ζ_m see ISO 23509.

$b_{2,eff}$ is the effective width of the contact pattern parallel to the pitch cone under a certain load. It should be derived from measurements or LTCA, at the preliminary design stage $b_{2,eff} = 0,85 \cdot b_2$ is a reasonable estimate.

In a second step, the facewidth b_v is defined according to [Formula \(A.22\)](#):

$$b_v = b_2 \cdot \frac{b_{v,eff}}{b_{2,eff}} \quad (\text{A.22})$$

A.2.5 Comparison of meshing conditions

The parallelogram as zone of action determined for the virtual cylindrical gear pair is now compared with the real contact lines and pattern calculated by a TCA of the bevel gear set. Both zones of action are projected into a plane vertical to the wheel axis and then superposed for illustration. Six such sample plots, derived from three gear sets with different offset values a , are arranged in [Table A.1](#), considering both flanks (drive side and coast side). As a reference, each little plot gives the axis of roll of virtual cylindrical gears and the lines of mean cone distances of pinion and wheel which intersect in the respective mean point P .

In addition, the parallelogram of the virtual zone of action contains three representative straight contact lines (bold lines). They fit angularly very well with the calculated curved contact lines which are drawn thicker where they form the contact pattern. Also, each of these calculated contact patterns is well covered in size and position by the parallelogram of the respective virtual cylindrical gear, which means that the equivalence of the meshing conditions between bevel gears and their virtual cylindrical gears is very good for a rating system.

It was found that the former ellipse, inscribed in the zone of action, produces no better results than the newly defined parallelogram. It seems that the major axis of the ellipse does not always have to be parallel to the axis of the virtual cylindrical gear, but should at least be turned by an angle, which would be very difficult to calculate.

Table A.1 — Exemplary zones of action of virtual cylindrical gear pairs and calculated contact patterns of the bevel gear sets in a projection parallel to the wheel axis

| Actual flank | Hypoid offset | | |
|---|--------------------|---------------------|---------------------|
| | $a = 0 \text{ mm}$ | $a = 15 \text{ mm}$ | $a = 30 \text{ mm}$ |
| Drive side | | | |
| Coast side | | | |
| Key 1 mean cone distance pinion 2 mean cone distance wheel 3 axis of roll | | | |

A.2.6 Determination of contact ratios, ε_v

For the determination of contact ratios, ε_v , [Formulae \(A.23\)](#) to [\(A.25\)](#) apply.

Transverse contact ratio, $\epsilon_{v\alpha}$:

$$\epsilon_{v\alpha} = g_{v\alpha} / p_{vet} \tag{A.23}$$

Face contact ratio, $\epsilon_{v\beta}$:

$$\epsilon_{v\beta} = \frac{b_{v,eff} \cdot \sin \beta_v}{\pi \cdot m_{mn}} \tag{A.24}$$

The transverse and face contact ratios calculated with [Formulae \(A.23\)](#) and [\(A.24\)](#) for the virtual cylindrical gear are determinant for the load capacity calculation. But it is possible that they deviate from the ratios calculated on the basis of the real dimensions of the bevel gears or on the basis of a TCA.

NOTE [Formula \(A.24\)](#) considers the effective facewidth and not the geometrical facewidth. Typically, this leads to lower contact ratios compared to calculations considering the geometrical facewidth.

Virtual contact ratio, $\epsilon_{v\gamma}$:

$$\epsilon_{v\gamma} = \epsilon_{v\alpha} + \epsilon_{v\beta} \tag{A.25}$$

A.2.7 Determination of the length of contact lines, l_b

When the tooth contact has been suitably developed, the full load contact should not extend beyond the boundary of the assumed parallelogram (see [Figure A.4](#)). Normally, the contact lines are shorter than they theoretically can be because of the crowning of the flanks in profile and lengthwise directions. This is considered with the correction factor C_{lb} which reduces the length of the contact lines by an elliptical function (see [Figure A.5](#)).

[Formulae \(A.26\)](#) to [\(A.36\)](#) shall be calculated, according to [Table A.2](#), for:

- a) the tip contact line with $f = f_t$;
- b) the middle contact line, l_{bm} , with $f = f_m$;
- c) the root contact line with $f = f_r$.

Table A.2 — Distance f of the tip, middle and root contact line in the zone of action

| | | Surface durability | Tooth root strength |
|-----------------------------|-------|---|--|
| $\epsilon_{v\beta} = 0$ | f_t | $-(p_{vet} - 0,5 \cdot p_{vet} \cdot \epsilon_{v\alpha}) \cdot \cos \beta_{vb} + p_{vet} \cdot \cos \beta_{vb}$ | $(p_{vet} - 0,5 \cdot p_{vet} \cdot \epsilon_{v\alpha}) \cdot \cos \beta_{vb} + p_{vet} \cdot \cos \beta_{vb}$ |
| | f_m | $-(p_{vet} - 0,5 \cdot p_{vet} \cdot \epsilon_{v\alpha}) \cdot \cos \beta_{vb}$ | $(p_{vet} - 0,5 \cdot p_{vet} \cdot \epsilon_{v\alpha}) \cdot \cos \beta_{vb}$ |
| | f_r | $-(p_{vet} - 0,5 \cdot p_{vet} \cdot \epsilon_{v\alpha}) \cdot \cos \beta_{vb} - p_{vet} \cdot \cos \beta_{vb}$ | $(p_{vet} - 0,5 \cdot p_{vet} \cdot \epsilon_{v\alpha}) \cdot \cos \beta_{vb} - p_{vet} \cdot \cos \beta_{vb}$ |
| $0 < \epsilon_{v\beta} < 1$ | f_t | $(p_{vet} - 0,5 \cdot p_{vet} \cdot \epsilon_{v\alpha}) \cdot \cos \beta_{vb} \cdot (1 - \epsilon_{v\beta}) + p_{vet} \cdot \cos \beta_{vb}$ | $(p_{vet} - 0,5 \cdot p_{vet} \cdot \epsilon_{v\alpha}) \cdot \cos \beta_{vb} \cdot (1 - \epsilon_{v\beta}) + p_{vet} \cdot \cos \beta_{vb}$ |
| | f_m | $-(p_{vet} - 0,5 \cdot p_{vet} \cdot \epsilon_{v\alpha}) \cdot \cos \beta_{vb} \cdot (1 - \epsilon_{v\beta})$ | $(p_{vet} - 0,5 \cdot p_{vet} \cdot \epsilon_{v\alpha}) \cdot \cos \beta_{vb} \cdot (1 - \epsilon_{v\beta})$ |
| | f_r | $-(p_{vet} - 0,5 \cdot p_{vet} \cdot \epsilon_{v\alpha}) \cdot \cos \beta_{vb} \cdot (1 - \epsilon_{v\beta}) - p_{vet} \cdot \cos \beta_{vb}$ | $(p_{vet} - 0,5 \cdot p_{vet} \cdot \epsilon_{v\alpha}) \cdot \cos \beta_{vb} \cdot (1 - \epsilon_{v\beta}) - p_{vet} \cdot \cos \beta_{vb}$ |
| $\epsilon_{v\beta} \geq 1$ | f_t | $+ p_{vet} \cdot \cos \beta_{vb}$ | $+ p_{vet} \cdot \cos \beta_{vb}$ |
| | f_m | 0 | 0 |
| | f_r | $- p_{vet} \cdot \cos \beta_{vb}$ | $- p_{vet} \cdot \cos \beta_{vb}$ |

NOTE Because of the symmetry of the contact area with respect to the point M , a contact line with the distance f has the same length compared to a contact line with the distance $-f$. Hence the sum of the length of the three considered contact lines is independent of the sign of distance f .

In this case, $f_{m(\text{macropitting})} = -f_{m(\text{tooth root})}$; $f_{r(\text{macropitting})} = -f_{r(\text{tooth root})}$ and $f_{t(\text{macropitting})} = -f_{t(\text{tooth root})}$. Together with the symmetry of load distribution according to ISO 10300-2:2023, Figure 2, this leads in

total to load sharing factors for macropitting, Z_{LS} , and ISO 10300-3:2023, 6.4.5 for tooth root, Y_{LS} , where $Y_{LS} = Z_{LS}^2$. Length of contact line, l_b :

If $f \geq f_{\max 0}$ then $l_b = 0$, else:

$$l_b = l_{b0} \cdot (1 - C_{lb}) \quad (\text{A.26})$$

for C_{lb} = correction factor, see [Formula \(A.36\)](#).

Coordinates of the ends of the contact line $x_{1,2}; y_{1,2}$ can be calculated with [Formulae \(A.27\)](#) to [\(A.31\)](#).

For bevel gears with $\beta_{vb} = 0$:

$$x_1 = 0 \quad (\text{A.27})$$

$$x_2 = b_{v,eff} \quad (\text{A.28})$$

For bevel gears with $\beta_{vb} > 0$:

$$x_1 = \frac{f \cdot \cos \beta_{vb} + \tan \beta_{vb} \cdot \left(f \cdot \sin \beta_{vb} + \frac{b_{v,eff}}{2} \right) + \frac{1}{2} \cdot (g_{v\alpha} + b_{v,eff} \cdot \tan \gamma)}{\tan \gamma + \tan \beta_{vb}} \quad (\text{A.29})$$

$$x_2 = \frac{f \cdot \cos \beta_{vb} + \tan \beta_{vb} \cdot \left(f \cdot \sin \beta_{vb} + \frac{b_{v,eff}}{2} \right) - \frac{1}{2} \cdot (g_{v\alpha} - b_{v,eff} \cdot \tan \gamma)}{\tan \gamma + \tan \beta_{vb}} \quad (\text{A.30})$$

where

$b_{v,eff}$ is the effective facewidth;

γ is the auxiliary angle for length of contact line calculation.

$$y_{1,2} = -x_{1,2} \cdot \tan \beta_{vb} + f \cdot \cos \beta_{vb} + \tan \beta_{vb} \cdot \left(f \cdot \sin \beta_{vb} + \frac{b_{v,eff}}{2} \right) \quad (\text{A.31})$$

Theoretical length of contact line, l_{b0} :

$$l_{b0} = \sqrt{(x_1 - x_2)^2 + (y_1 - y_2)^2} \quad (\text{A.32})$$

The maximum distances from the middle contact line are calculated according to [Figure A.4](#):

$$f_{\max B} = \frac{1}{2} \cdot [g_{v\alpha} + b_{v,eff} \cdot (\tan \gamma + \tan \beta_{vb})] \cdot \cos \beta_{vb} \quad (\text{A.33})$$

$$f_{\max 0} = \frac{1}{2} \cdot [g_{v\alpha} - b_{v,eff} \cdot (\tan \gamma + \tan \beta_{vb})] \cdot \cos \beta_{vb} \quad (\text{A.34})$$

with

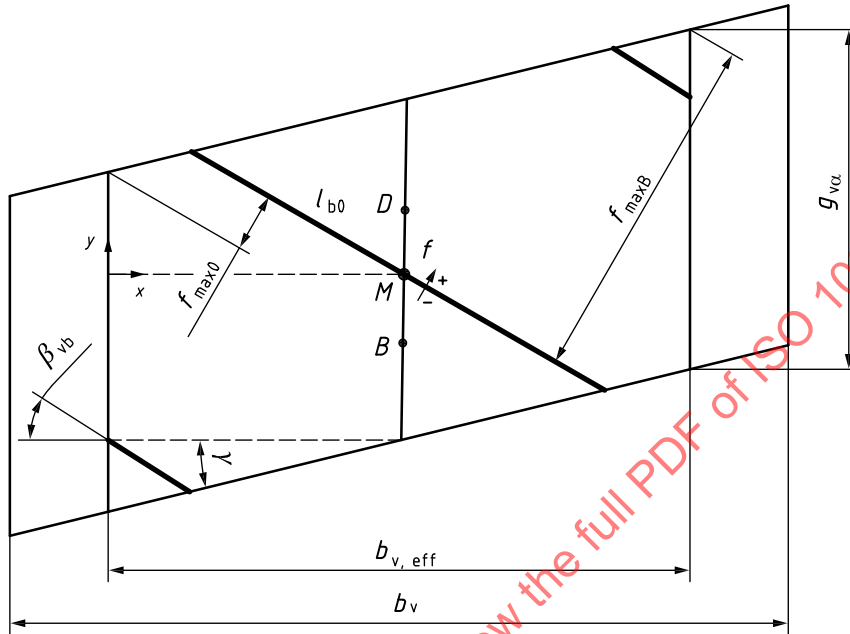
$$\tan \gamma = \tan \gamma' / \cos \alpha_{vet} \quad (\text{A.35})$$

If $f_{\max B} > f_{\max 0}$: $f_{\max} = f_{\max B}$ else $f_{\max} = f_{\max 0}$.

Correction factor, C_{lb} :

$$C_{lb} = \sqrt{\left(1 - \left(\frac{f}{f_{max}}\right)^2\right) \cdot \left(1 - \sqrt{\frac{b_{v,eff}}{b_v}}\right)^2} \tag{A.36}$$

Figure A.4 shows the general definitions of values for calculating the theoretical length of lines of contact, l_{b0} .



Key

- D outer point of single contact
- M centre of the zone of action
- B inner point of single contact

Figure A.4 — General definition of length of contact lines

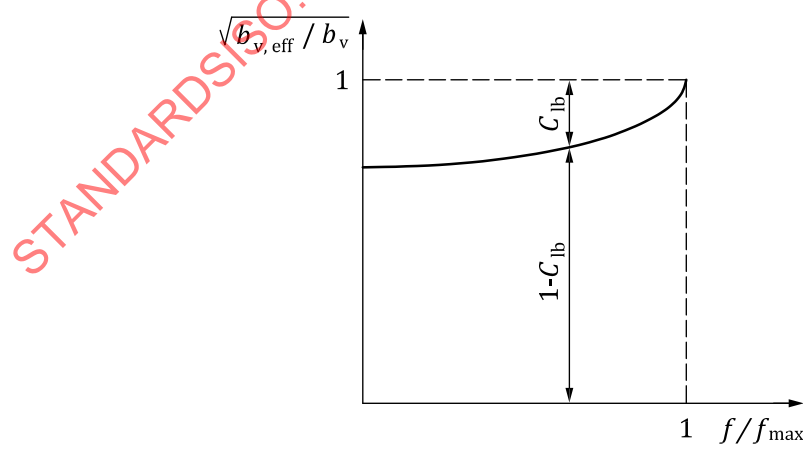


Figure A.5 — Correction factor, C_{lb}

A.2.8 Determination of the radius of relative curvature, ρ_{rel} for the contact stress calculation

Radius of relative curvature vertical to the contact line, ρ_{rel} , shall be calculated according to [Formulae \(A.37\)](#) to [\(A.40\)](#):

$$\rho_{\text{rel}} = |\rho_t| \cdot (\cos \beta_B)^2 \quad (\text{A.37})$$

Inclination angle of contact line, β_B :

$$\beta_B = \arctan(\tan \beta_v \cdot \sin \alpha_e) \quad (\text{A.38})$$

where

$\alpha_e = \alpha_{eD}$ for drive side (see ISO 23509);

$\alpha_e = \alpha_{eC}$ for coast side (see ISO 23509).

Radius of relative curvature in normal section at the mean point, ρ_t ; see Reference [4]:

a) Drive side:

$$\rho_t = \left[\frac{1}{\cos \alpha_{nD} \cdot (\tan \alpha_{nD} - \tan \alpha_{\text{lim}}) + \tan \zeta_{\text{mp}} \cdot \tan \beta_B} \cdot \frac{\cos \beta_{m1} \cdot \cos \beta_{m2}}{\cos \zeta_{\text{mp}}} \cdot \left(\frac{1}{R_{m2} \cdot \tan \delta_2} + \frac{1}{R_{m1} \cdot \tan \delta_1} \right) \right]^{-1} \quad (\text{A.39})$$

b) Coast side:

$$\rho_t = \left[\frac{1}{\cos \alpha_{nC} \cdot (\tan(-\alpha_{nC}) - \tan \alpha_{\text{lim}}) - \tan \zeta_{\text{mp}} \cdot \tan \beta_B} \cdot \frac{\cos \beta_{m1} \cdot \cos \beta_{m2}}{\cos \zeta_{\text{mp}}} \cdot \left(\frac{1}{R_{m2} \cdot \tan \delta_2} + \frac{1}{R_{m1} \cdot \tan \delta_1} \right) \right]^{-1} \quad (\text{A.40})$$

A.3 Data of virtual cylindrical gear in normal section (suffix vn)

For the data of virtual cylindrical gear in normal section, [Formulae \(A.41\)](#) to [\(A.46\)](#) apply.

Number of teeth z_{vn} of virtual spur gears:

$$z_{\text{vn}1} = \frac{z_{v1}}{\cos^2 \beta_{vb} \cdot \cos \beta_v} \quad (\text{A.41})$$

$$z_{\text{vn}2} = u_v \cdot z_{\text{vn}1} \quad (\text{A.42})$$

Reference diameter d_{vn} :

$$d_{\text{vn}1,2} = \frac{d_{v1,2}}{\cos^2 \beta_{vb}} = z_{\text{vn}1,2} \cdot m_{\text{mn}} \quad (\text{A.43})$$

Tip diameter d_{van} :

$$d_{\text{van}1,2} = d_{\text{vn}1,2} + d_{\text{va}1,2} - d_{\text{v}1,2} = d_{\text{vn}1,2} + 2 \cdot h_{\text{am}1,2} \quad (\text{A.44})$$

Base diameter d_{vbn} :

$$d_{\text{vbn}1,2} = d_{\text{vn}1,2} \cdot \cos \alpha_e = z_{\text{vn}1,2D,C} \cdot m_{\text{mn}} \cdot \cos \alpha_e \quad (\text{A.45})$$

where

$\alpha_e = \alpha_{eD}$ for drive side (see ISO 23509);

$\alpha_e = \alpha_{eC}$ for coast side (see ISO 23509).

Profile contact ratio $\varepsilon_{v\alpha n}$:

$$\varepsilon_{v\alpha n} = \varepsilon_{v\alpha} / (\cos \beta_{vb})^2 \tag{A.46}$$

Hypoid gears with different effective pressure angles for drive and coast side have different virtual cylindrical gears in normal section. Therefore, z_{vn} , d_{van} and d_{vbn} shall be calculated separately for drive flank (suffix D) and coast flank (suffix C).

A.4 Determination of local geometry data of virtual cylindrical gear

A.4.1 General

In addition to the calculation at the design point, there is the possibility of local calculations at points along the path of contact of the virtual cylindrical gear.

A.4.2 Transverse path of contact

For local calculation along the transverse path of contact, the coordinate g_Y is introduced with its origin in the pitch point C, i.e. $g_Y(C) = 0$, as shown in [Figure A.6](#).

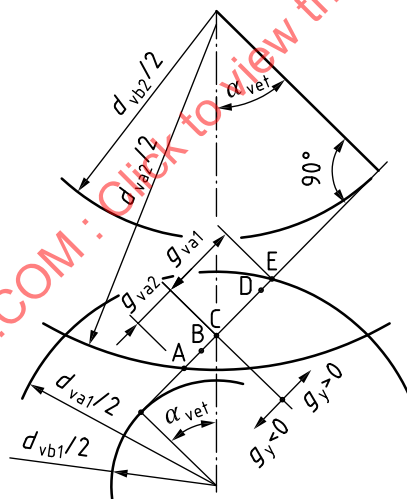


Figure A.6 — Transverse path of contact

Towards the pinion tip, g_Y is defined as positive and towards the pinion root it is defined as negative. In the boundary points A and E on the transverse path of contact, g_Y is determined by [Formulae \(A.47\)](#) and [\(A.48\)](#):

$$g_Y(A) = -g_{va2} \tag{A.47}$$

$$g_Y(E) = g_{va1} \quad (A.48)$$

The length of path of contact of virtual cylindrical gears in transverse section can be derived from [Formula \(A.49\)](#):

$$g_{v\alpha} = g_{va1} + g_{va2} = \frac{1}{2} \cdot \left[\left(\sqrt{d_{va1}^2 - d_{vb1}^2} - d_{v1} \cdot \sin \alpha_{vet} \right) + \left(\sqrt{d_{va2}^2 - d_{vb2}^2} - d_{v2} \cdot \sin \alpha_{vet} \right) \right] \quad (A.49)$$

$g_{v\alpha}$ is the length of path of contact of virtual cylindrical gear in transverse section;

g_{va} is the length of tip path of contact;

α_{vet} is the transverse pressure angle of virtual cylindrical gear;

d_v is the reference diameter of virtual cylindrical gear;

d_{va} is the tip diameter of virtual cylindrical gear;

d_{vb} is the base diameter of virtual cylindrical gear.

Between the two boundary points the length of the transverse path of contact can be subdivided in a number of sections i which are specified by the user. For bevel gears with mean spiral angle zero ($\beta_m = 0$) calculations are not performed at the tip and root points to avoid infinity values in some of the following formulae. [Formula \(A.50\)](#) is used to calculate the coordinate g_Y (Y) of a contact point Y on the transverse path of contact using auxiliary variable k_s to exclude tip and root boundary points for bevel gear with mean spiral angle zero ($\beta_m = 0$).

$$g_Y(Y) = g_Y(A) + k_s \cdot g_{v\alpha} + Y \cdot \frac{(1 - 2 \cdot k_s) \cdot g_{v\alpha}}{i} \text{ with } Y = 0 \dots i \quad (A.50)$$

where

$k_s = 0$ for bevel gears with $\beta_{vb} > 0$;

$k_s = 0,001$ for bevel gears with $\beta_{vb} = 0$.

NOTE In [Formulae \(A.51\)](#) to [\(A.63\)](#), g_Y is a function of Y ($g_Y = g_Y(Y)$).

A.4.3 Length of contact lines

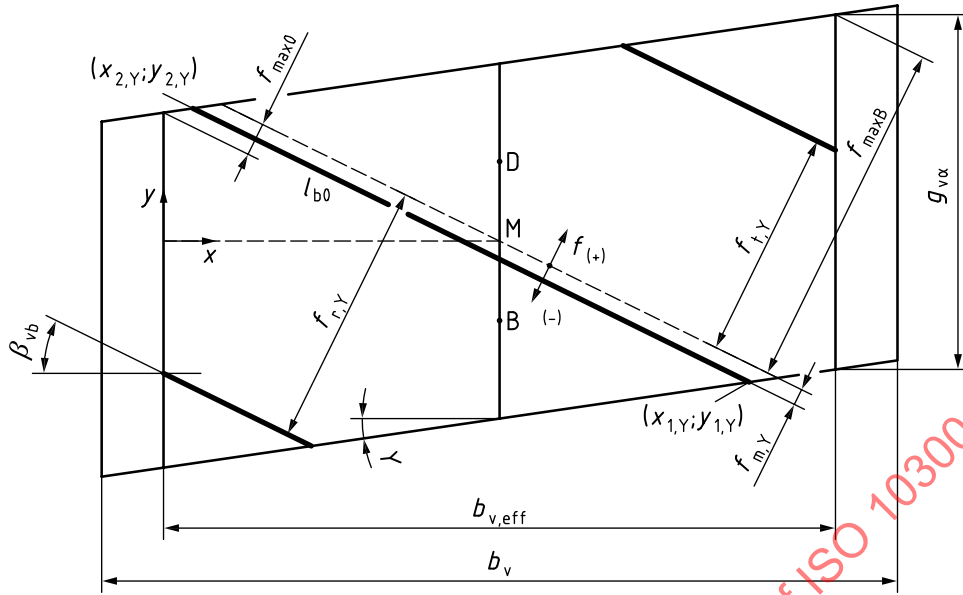


Figure A.7 — General definition of length of contact lines for local geometry data

Distance of the tip, $f_{t,Y}$, middle, $f_{m,Y}$ and root, $f_{r,Y}$, contact line in the zone of action can be calculated by using [Formulae \(A.51\) to \(A.53\)](#).

$$f_{m,Y} = (g_{va2} - g_{v\alpha} / 2 + g_Y) \cdot \cos \beta_{vb} \tag{A.51}$$

$$f_{t,Y} = f_{m,Y} + p_{vet} \cdot \cos \beta_{vb} \tag{A.52}$$

$$f_{r,Y} = f_{m,Y} - p_{vet} \cdot \cos \beta_{vb} \tag{A.53}$$

where

β_{vb} is the helix angle at base circle;

p_{vet} is the transverse base pitch.

If the absolute value of $f_{m,Y}$, $f_{t,Y}$ or $f_{r,Y}$ is larger than f_{max} , the contact line is outside the zone of action. Therefore the length of contact line $l_{b,Y}$ [see [Formula \(A.59\)](#)] and $l_{b0,Y}$ [see [Formula \(A.60\)](#)] is set to zero. Otherwise, $l_{b,Y}$ and $l_{b0,Y}$ are calculated with [Formulae \(A.54\) to \(A.61\)](#).

Coordinates of the ends of the contact line $x_{1,2,Y}; y_{1,2,Y}$ can be calculated with [Formulae \(A.54\) to \(A.58\)](#).

For bevel gears with $\beta_{vb} = 0$:

$$x_{1,Y} = 0 \tag{A.54}$$

$$x_{2,Y} = b_{v,eff} \tag{A.55}$$

For bevel gears with $\beta_{vb} > 0$:

$$x_{1,Y} = \frac{f_Y \cdot \cos \beta_{vb} + \tan \beta_{vb} \cdot \left(f_Y \cdot \sin \beta_{vb} + \frac{b_{v,eff}}{2} \right) + \frac{1}{2} \cdot (g_{v\alpha} + b_{v,eff} \cdot \tan \gamma)}{\tan \gamma + \tan \beta_{vb}} \tag{A.56}$$

$$x_{2,Y} = \frac{f_Y \cdot \cos \beta_{vb} + \tan \beta_{vb} \cdot \left(f_Y \cdot \sin \beta_{vb} + \frac{b_{v,eff}}{2} \right) - \frac{1}{2} \cdot (g_{v\alpha} - b_{v,eff} \cdot \tan \gamma)}{\tan \gamma + \tan \beta_{vb}} \quad (A.57)$$

where

$b_{v,eff}$ is the effective facewidth;

γ is the auxiliary angle for length of contact line calculation.

$$y_{1,2,Y} = -x_{1,2,Y} \cdot \tan \beta_{vb} + f_Y \cdot \cos \beta_{vb} + \tan \beta_{vb} \cdot \left(f_Y \cdot \sin \beta_{vb} + \frac{b_{v,eff}}{2} \right) \quad (A.58)$$

$x_{1,2,Y}$ and $y_{1,2,Y}$ shall be calculated with $f_{m,Y}$, $f_{t,Y}$ or $f_{r,Y}$ for three contact lines.

Length of contact line $l_{b,Y}$ shall be calculated with [Formulae \(A.59\)](#) to [\(A.61\)](#).

$$l_{b,Y} = l_{b0,Y} \cdot (1 - C_{lb,Y}) \quad (A.59)$$

where

$$l_{b0,Y} = \sqrt{(x_{1,Y} - x_{2,Y})^2 + (y_{1,Y} - y_{2,Y})^2} \quad (A.60)$$

$l_{b0,Y}$ is the theoretical length of contact line;

$$C_{lb,Y} = \sqrt{\left(1 - \left(\frac{f_Y}{f_{max}} \right)^2 \right) \cdot \left(1 - \sqrt{\frac{b_{v,eff}}{b_v}} \right)^2} \quad (A.61)$$

C_{lb} is the correction factor for the length of contact lines;

b_v is the facewidth;

f_{max} is the maximum distance to middle contact.

A.4.4 Local equivalent radius of curvature, $\rho_{rel,Y}$

Local equivalent radius of curvature vertical to the contact line in the contact point Y, $\rho_{rel,Y}$, shall be calculated with [Formulae \(A.62\)](#) and [\(A.63\)](#).

$$\rho_{rel,Y} = \rho_{rel} \cdot \frac{1}{X_Y^2} \quad (A.62)$$

where ρ_{rel} is the equivalent radius of curvature vertical to the contact line;

$$X_Y = \frac{\tan \alpha_{\text{vet}}}{\sqrt{\frac{(d_{v1}/2 \cdot \sin \alpha_{\text{vet}} + g_Y)}{d_{vb1}/2}} \cdot \sqrt{\frac{(d_{v2}/2 \cdot \sin \alpha_{\text{vet}} - g_Y)}{d_{vb2}/2}}} \quad (\text{A.63})$$

X_Y is the curvature factor.

STANDARDSISO.COM : Click to view the full PDF of ISO 10300-1:2023

Annex B (normative)

Calculation of virtual cylindrical gears — Method B2

B.1 General

[Clause B.2](#) contains the geometric relations for generating the virtual cylindrical gear data required for bevel gear load capacity calculations when using method B2. The initial bevel gear data necessary for the virtual gear calculation should conform with ISO 23509. A base unit of one diametral pitch, $1,0/m_{et2}$, is used in the calculations.

[B.3](#) and [B.4](#) contain illustrations that demonstrate the procedure used to evaluate tooth loading and its distribution.

B.2 Approximate values for application factors

For the following approximate values for application factors, [Formulae \(B.1\)](#) to [\(B.26\)](#) shall be used.

Relative virtual facewidth:

$$b_{v,rel} = \frac{b_2}{m_{et2}} \quad (B.1)$$

Relative mean back cone distance:

$$R_{mpt1,2} = \frac{R_{m1,2} \cdot \tan \delta_{1,2}}{m_{et2}} \quad (B.2)$$

Angle between direction of contact and the pitch tangent (for hypoid gears only):

$$\cot(\zeta_{mp} - \lambda) = \cot \zeta_{mp} \cdot \left(1,0 + \frac{z_1 \cdot \cos \delta_2}{z_2 \cdot \cos \delta_1 \cdot \cos \zeta_{mp}} \right) \quad (B.3)$$

for ζ_{mp} = pinion offset angle in pitch plane, see ISO 23509:2016, Formula (114).

Face contact ratio:

a) for bevel gears:

$$\varepsilon_{v\beta} = b_2 \cdot \sin \beta_{m2} / (\pi \cdot m_{mn}) \quad (B.4)$$

b) for hypoid gears:

$$\varepsilon_{v\beta} = \left[\frac{\cos \beta_{m2}}{\cot(\zeta_{mp} - \lambda)} + \sin \beta_{m2} \right] \cdot \frac{b_2}{\pi \cdot m_{mn}} \quad (B.5)$$